2.0 GEOLOGY, GEOPHYSICS AND PETROPHYSICS

The **Sable Offshore Energy Project** will produce natural gas from porous sandstone reservoirs which lie deep under the sea floor of the Sable Island area. This chapter is a description of these reservoirs, and is divided into two parts.

The first part is a regional overview. This includes a general introduction to the geological history of the Sable area. It also describes the methodology used to determine the size and nature of the reservoirs.

The second part is a field-by-field description of gas accumulations currently included in the Project. It contains a summary of the structure, stratigraphic setting, and gas in place (GIP) estimates for each of the six **Sable Offshore Energy Project** fields: Thebaud, Venture, North Triumph, South Venture, Glenelg, and Alma.

2.1 Geological Interpretation and Reservoir Description

2.1.1 Regional Structural Setting

The Scotian Shelf is a narrow (125 to 225 kilometre wide) north-easterly trending continental margin which extends 800 kilometres from the Northeast Channel to the Laurentian Channel. **Figure 2.1.1.1** illustrates the location of the Scotian Shelf.

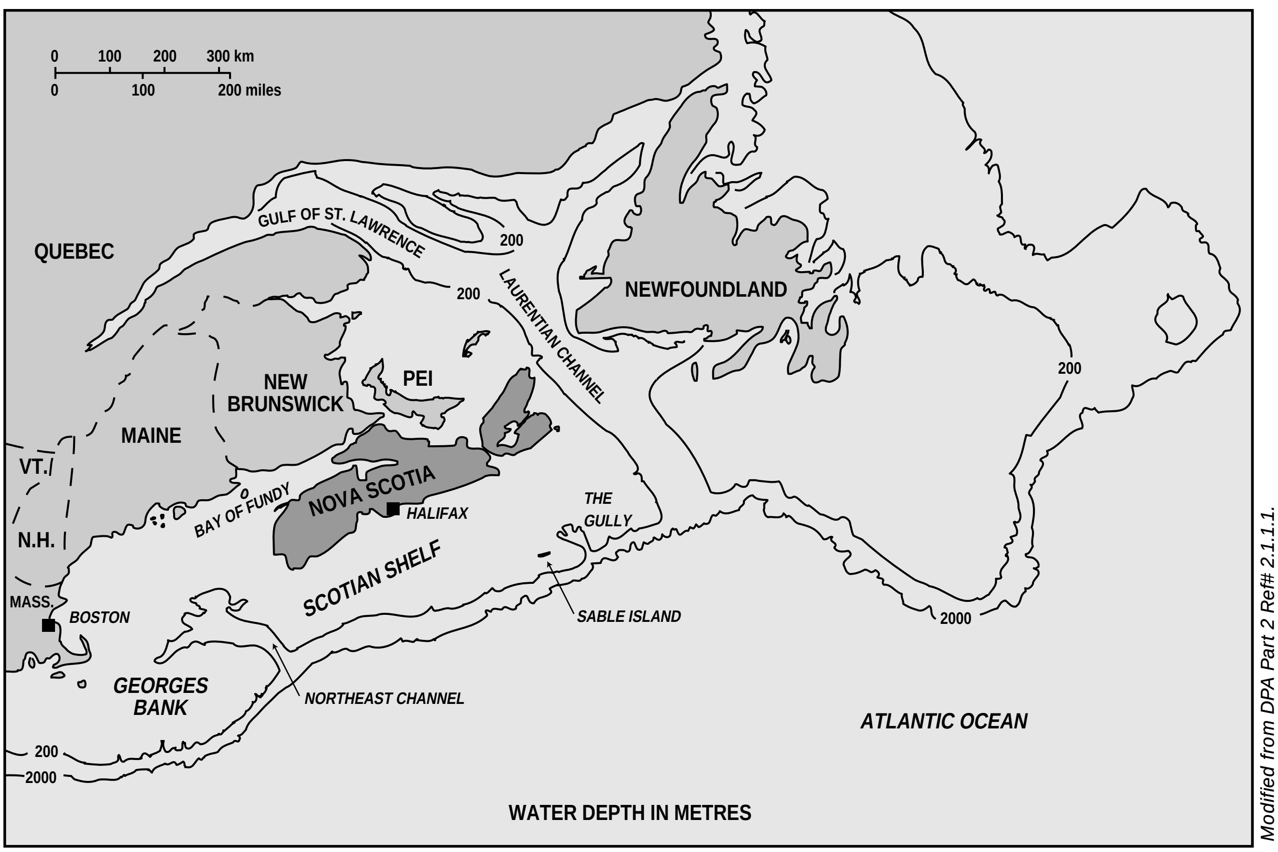

Figure 2.1.1.1: Location of the Scotian Shelf

The post-Palaeozoic geologic history of this area consists of continental extension and rifting, followed by ocean opening and the development of a passive continental margin. Extension faulting during the rifting stage, beginning in the Late Triassic and terminating in the Early Jurassic with the separation of Africa from North America, created a network of basement ridges and basins, collectively termed the ‘Scotian Basin.’ The gas fields lie within one of these basins, the ‘Sable Subbasin.’ **Figure 2.1.1.2** illustrates the tectonic elements of the Scotian Basin. A detailed discussion of the structural setting of the Scotian Basin is found in Part Two (**DPA - Part 2, Ref. # 2.1.1.1. through 2.1.1.5**).

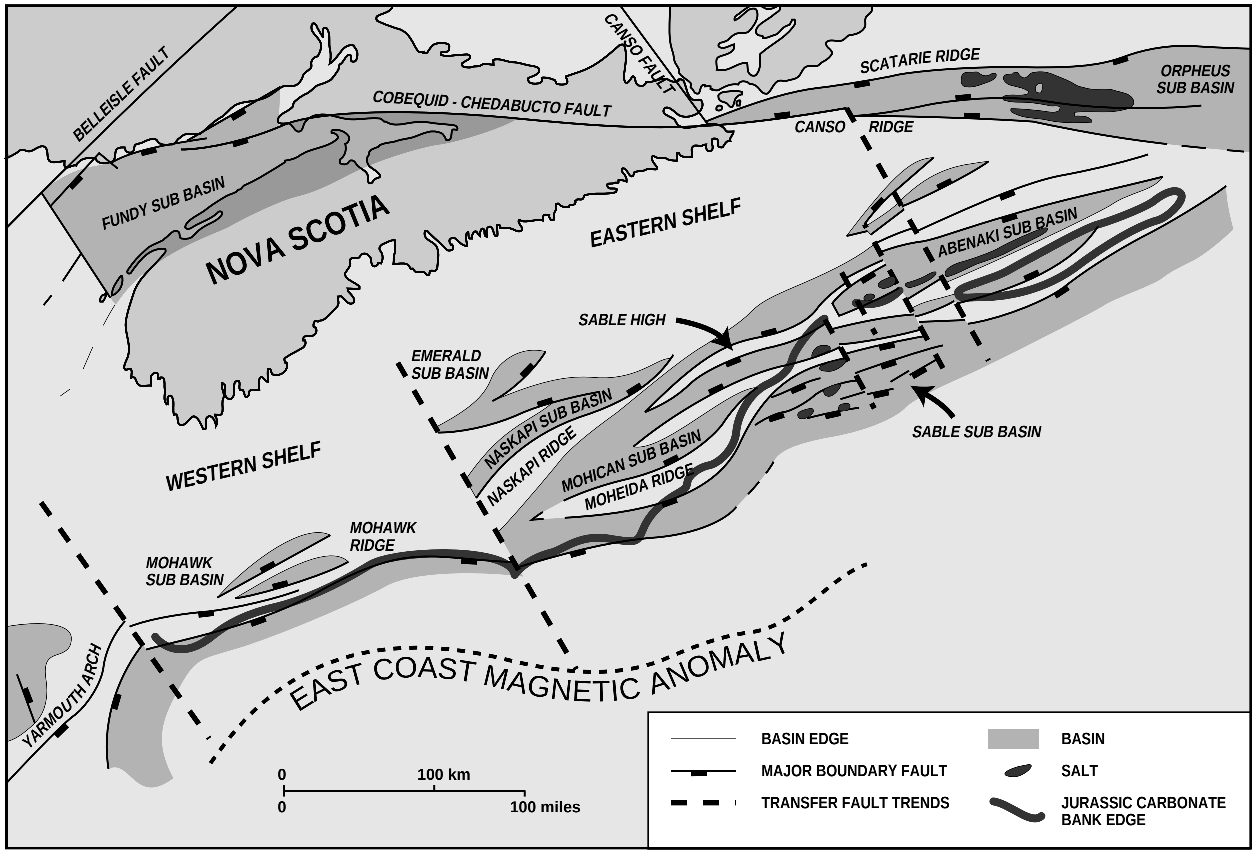

Modified from DPA Part 2 Ref# 2.1.1.5.

Figure 2.1.1.2: Tectonic Elements of the Scotian Basin

2.1.2 Regional Stratigraphy

The stratigraphy of the Scotian Shelf consists of two parts: a basement of complexly structured Cambro-Ordovician metasediments and Devonian granites, and a cover of Mesozoic-Cenozoic sediments. **Figure 2.1.2.1** illustrates the generalized stratigraphy of the Scotian Shelf.

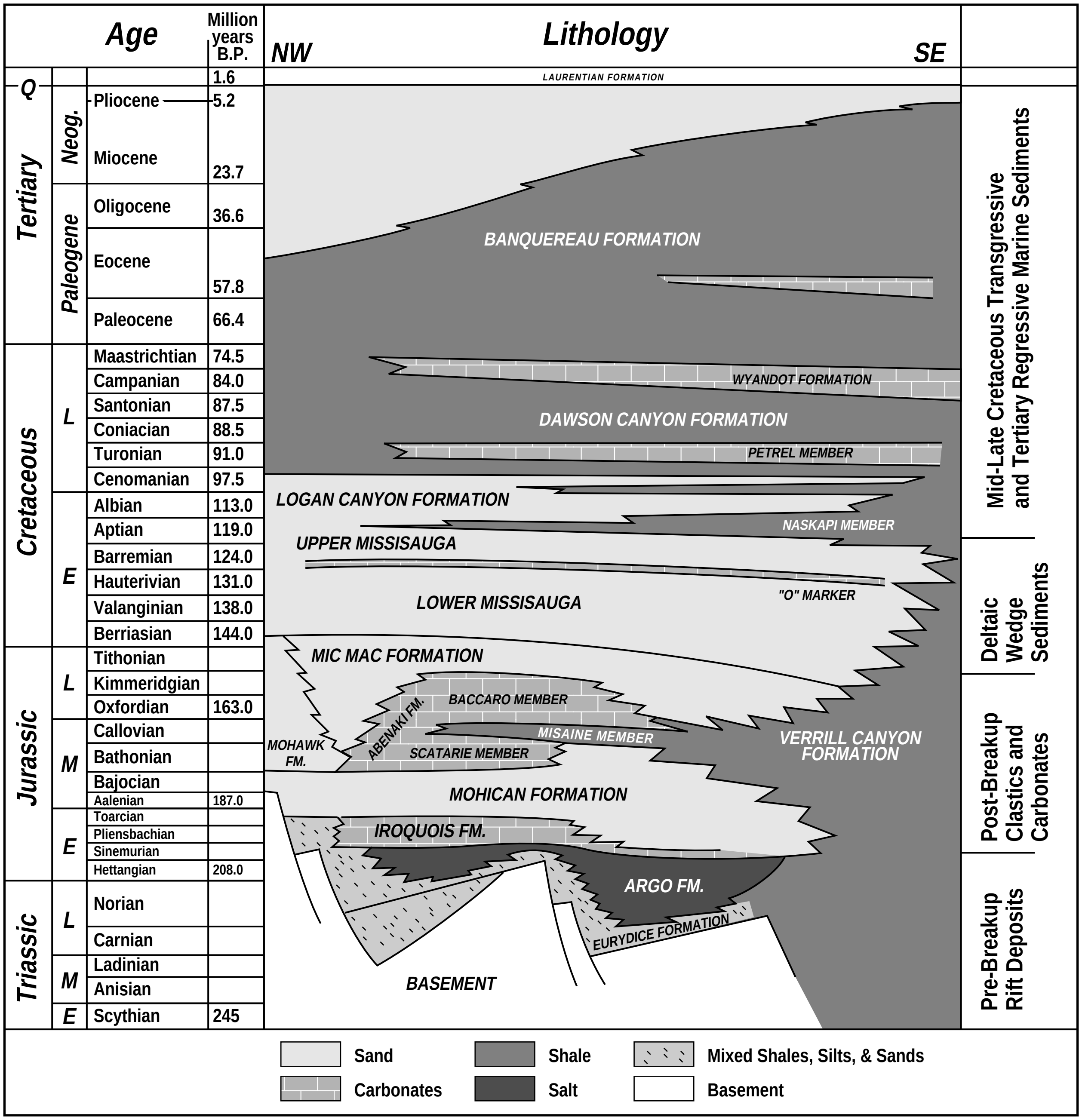

Modified from DPA Part 2 Ref# 2.1.1.1.

Figure 2.1.2.1: Generalized Stratigraphy of the Scotian Shelf

During the Late Triassic-Early Jurassic rifting phase, grabens and half grabens formed by basement faulting were initially filled with synrift continental clastics (Eurydice Formation). Subsequent deposition of evaporites (Argo Formation) and dolomites (Iroquois Formation) record the gradual change from non-marine to marine conditions associated with the opening of the North Atlantic.

With marine transgression and the onset of open marine conditions, a major carbonate bank, the Abenaki Formation, developed at the Jurassic shelf edge. This marked a distinct break in slope. There was an abrupt change from shallow water marine shelf environments in the north and west to deepwater environments to the south and east. Deep water marine shales, in the lower Verrill Canyon Formation, were deposited seaward of the shelf edge carbonate bank. Shallow shelf calcareous sands, shales and carbonate muds (Mic Mac Formation) were deposited landward of the shelf edge. In the Sable Subbasin, local rapid structural downwarping combined with clastic influx precluded the development of the carbonate bank. A small Mic Mac delta system developed in this area.

There was continued outpouring of clastic sediments during the Late Jurassic-Early Cretaceous. This was fed by a major continental drainage system and formed the Sable Delta complex (**D.P.A. Part 2, Ref. 2.1.2.2**). The Sable Subbasin was rapidly filled with sand rich delta front and delta plain sediments (Missisauga Formation) and prodelta shales (Verrill Canyon Formation). **Figure 2.1.2.2** illustrates the various depositional components of a typical, modern delta system; deposits of the sand rich shoreface and strand plain environments form the best quality reservoirs. **Figure 2.1.2.3** is a paleogeographic map showing the distribution of the Sable Delta complex, the sandstones of which form the reservoirs in the Project fields. This deltaic sequence was subsequently transgressed and capped by a thick marine shale unit (Naskapi Shale).

Modified from DPA Part 2 Ref. 2.1.1.6.

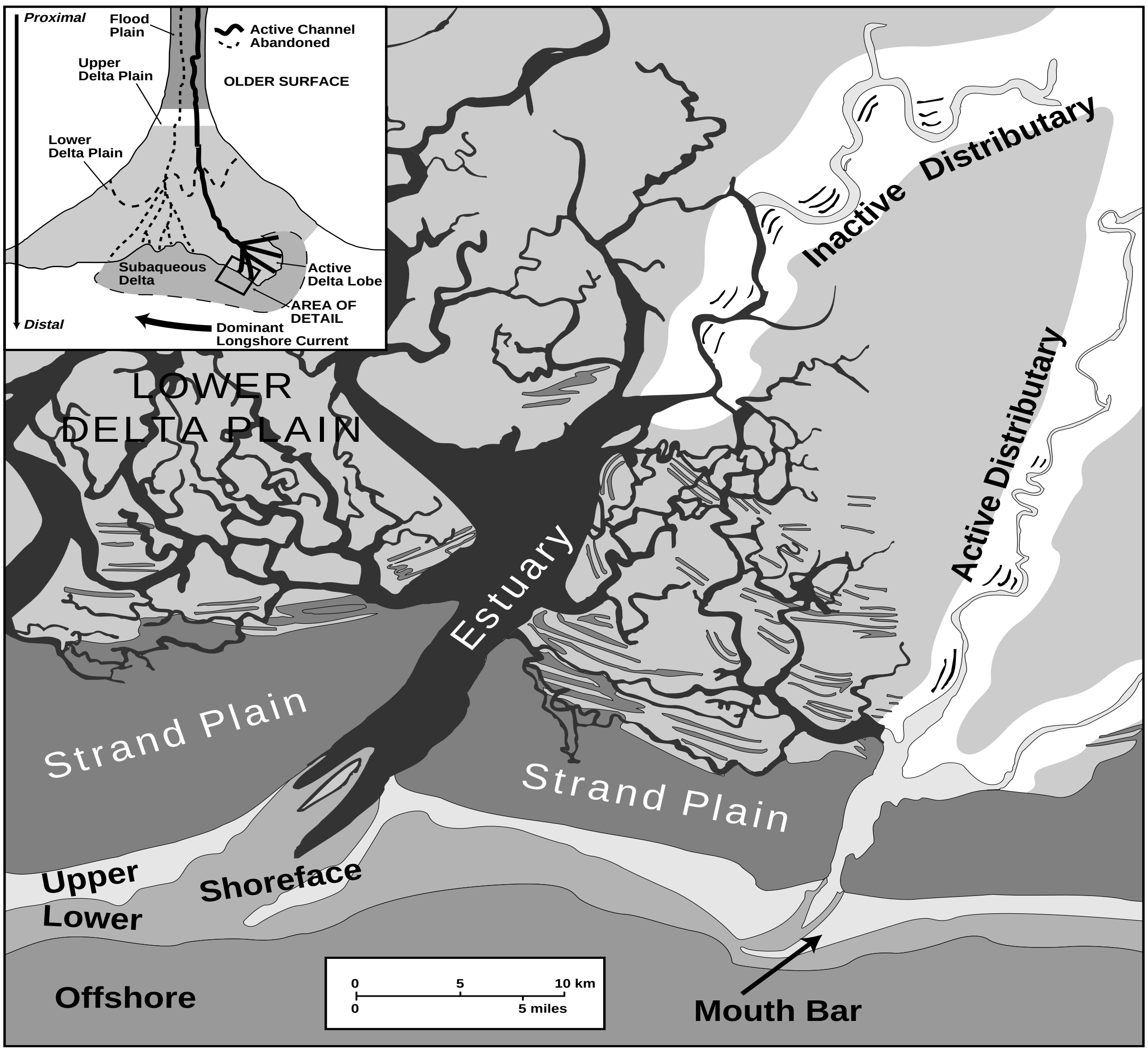

Modified from DPA Part 2 Ref# 2.1.5.1.

Figure 2.1.2.2 : Depositional Components of a Delta System

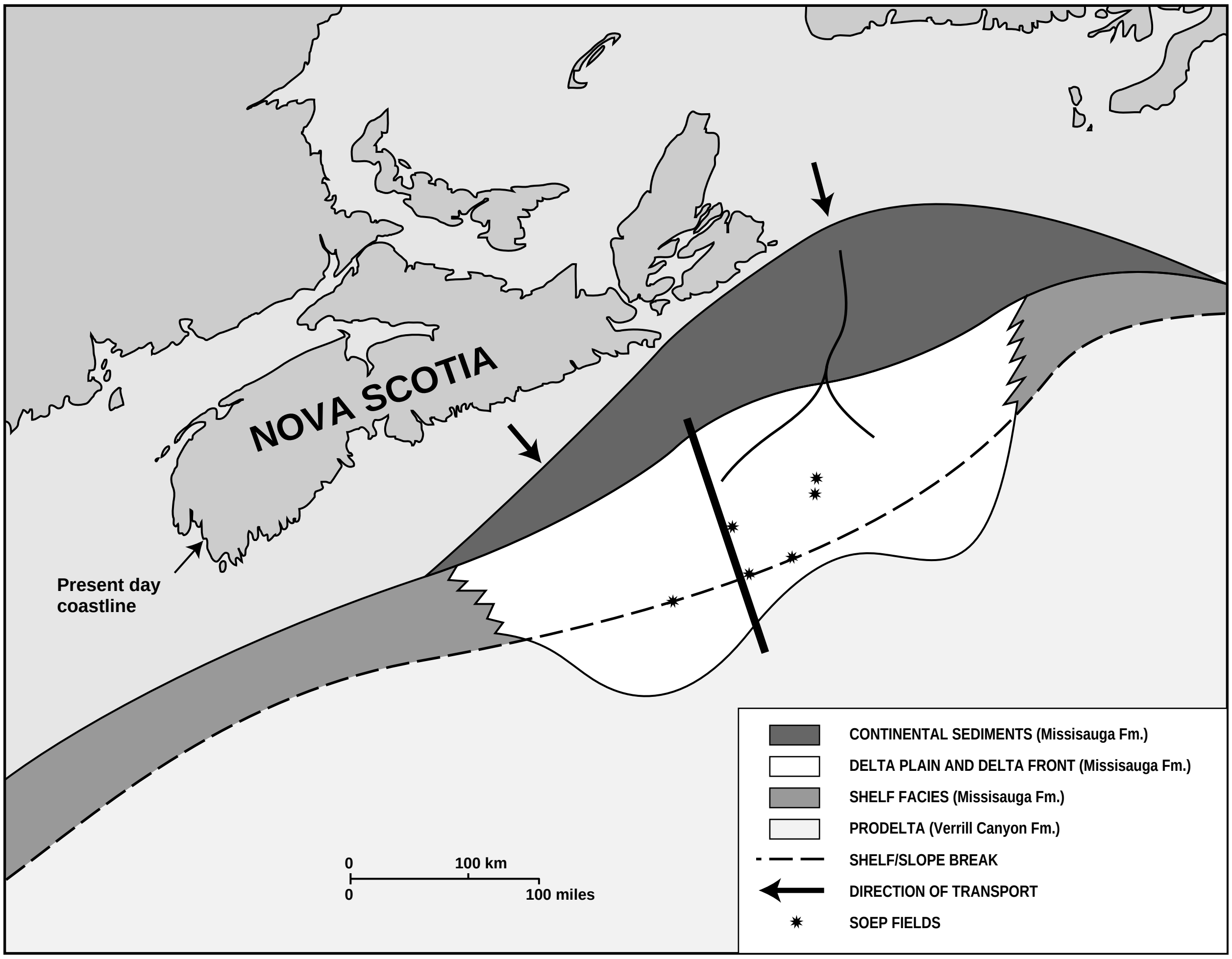

Modified from DPA Part 2 Ref# 2.1.1.1.

Figure 2.1.2.3: Paleogeographic Map of Sable Island Delta complex (Early Cretaceous Time). Line of Section in Figure 2.1.3.1(b) is indicated.

Late-stage passive margin development during the remainder of Early Cretaceous time was marked by a series of landward backstepping, shallow marine progradational lobes (Logan Canyon Formation) which interfinger with distal equivalent marine shales.

During the final stages of passive margin development, Late Cretaceous marine transgression deposited the Petrel limestone. This was followed by deep water deposition of Dawson Canyon Formation shales, Wyandot Formation chalky limestone, and Tertiary clastics of the Banquereau Formation. A more thorough description of the stratigraphy of the Scotian Basin is found in Part Two (**DPA - Part 2, Ref. # 2.1.1.1 through 2.1.1.5, 2.1.2.1 and 2.1.2.2**).

2.1.3 Source and Trapping of Hydrocarbons

The Verrill Canyon shales, depositionally distal marine equivalents of the deltaic Mic Mac and Missisauga Formations, are considered the most likely source of gas and condensate in the Sable Subbasin (**DPA - Part 2, Ref. # 2.1.3.1**). They are described as lipid-poor, gas-prone, low-total organic content (TOC), type III (terrestrial) source rocks (**DPA - Part 2, Ref. # 2.1.3.2 through 2.1.3.4**). Growth faults were active during and after deposition of the Mic Mac and Missisauga formations; anticlines associated with growth faulting formed traps for migrating hydrocarbons. All the **Sable Offshore Energy Project** fields occur in such growth fault related structures. **Figure 2.1.3.1(a)** illustrates the mechanism of growth fault development. **Figure 2.1.3.1(b)** illustrates the presence of growth faults in a north/south seismic line across the Sable Subbasin, and shows a strong relationship between hydrocarbon accumulations and growth fault-related anticlines.

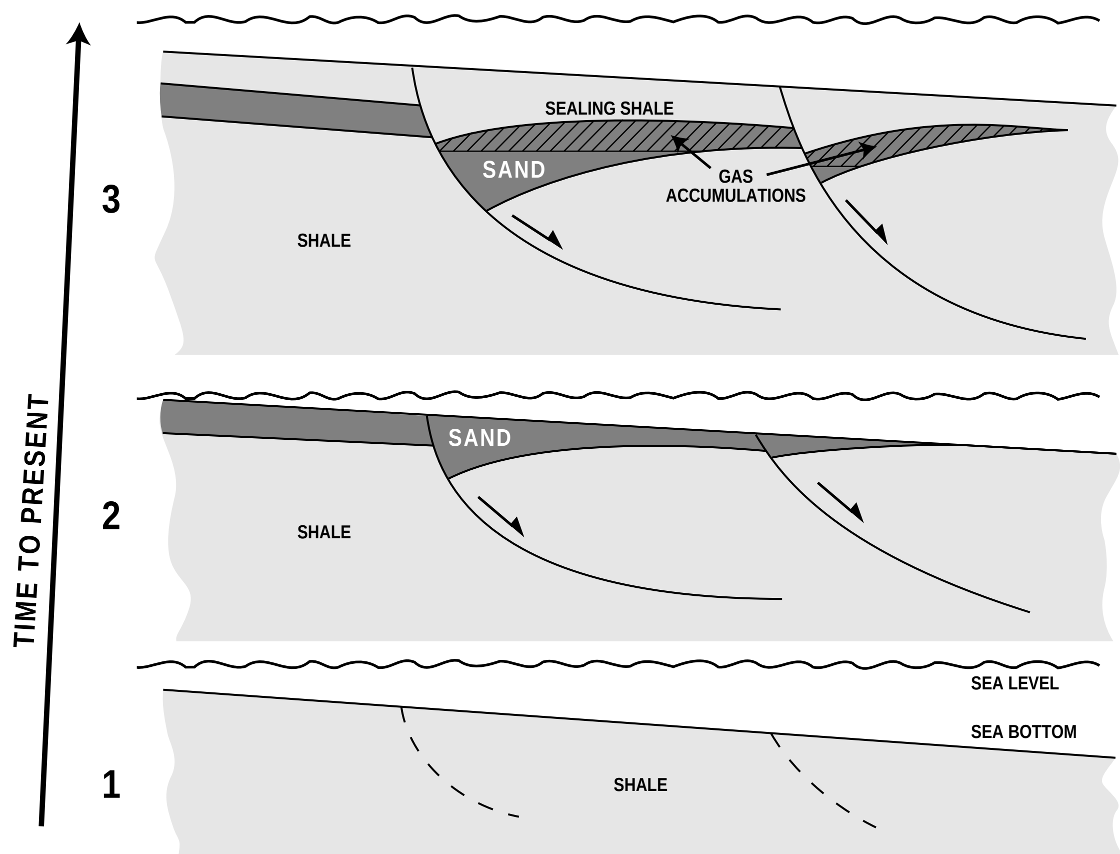

Time 1: Represents shale deposition distal (in front of) deltaic sand, prior to development of growth faults. Future growth fault locations shown by dashed lines. Note listric (curved) nature of fault lines.

Time 2: Sandy deltaic deposits have advanced into the area. Loading by these sediments (coupled with gravity induced extension) results in the development of listric growth faults. Movement along these faults causes sand deposition to be concentrated in the space created in the downthrown block immediately adjacent to the faults. Movement on the listric faults also causes rotation of the downthrown block, resulting in the formation of 'roll-over' anticlines.

Time 3: Delta-switching and/or rise in sea level causes sand deposition to be replaced by shale deposition. These pro-delta shales act as seals, and trap gas migrating into reservoir quality sandstones in the roll-over anticlines beneath.

Figure 2.1.3.1(a) Sequential Development of Growth Faults

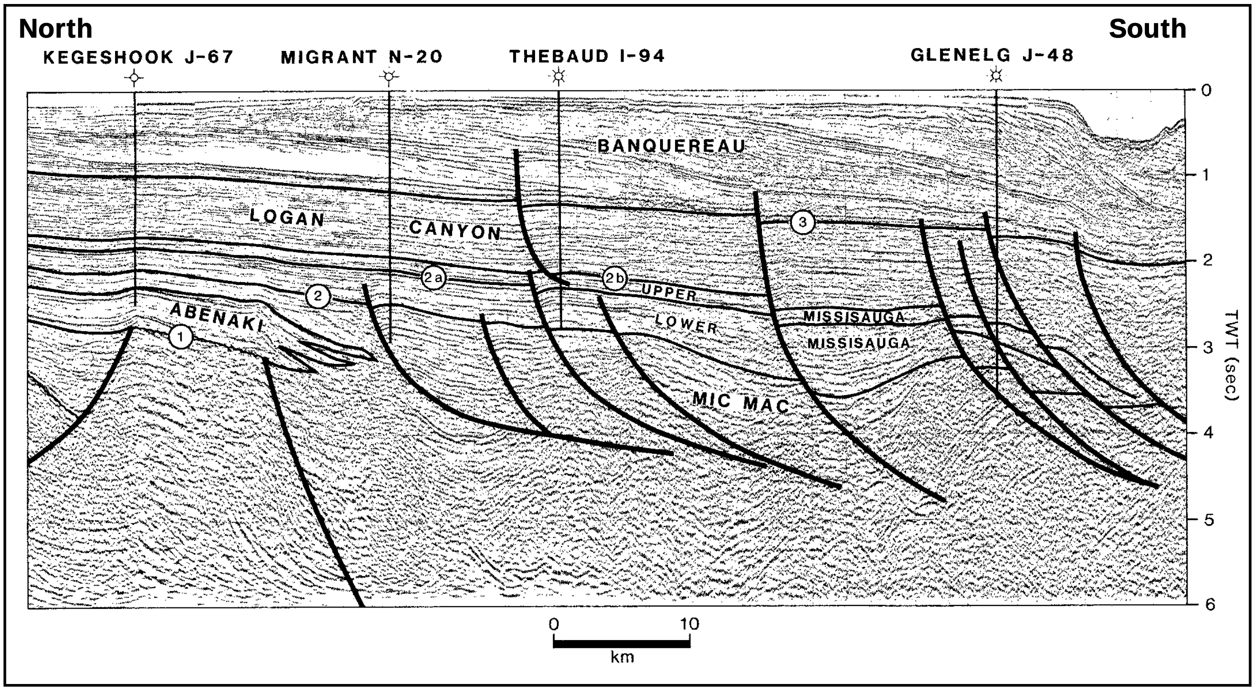

Modified from DPA Part 2 Ref# 2.1.1.5.

Figure 2.1.3.1(b) North-South Seismic Line Showing Growth Faults in the Sable Subbasin. Note that many growth fault-related anticlines contain hydrocarbons. Circled numbers refer to seismic events discussed at length in DPA Part 2, Ref. # 2.1.1.5. Line of Section is shown in Figure 2.1.2.3.

Gas accumulations in the Sable Subbasin occur in both hydropressured and overpressured reservoirs. Overpressured reservoirs have a subsurface pore-fluid pressure greater than that of normal hydrostatic pressure. The North Triumph, Glenelg and Alma fields are hydropressured. The shallower reservoirs of the Thebaud, Venture and South Venture fields are also hydropressured, while the deeper reservoirs in these fields are overpressured. Recent basin modeling studies **(DPA - Part 2 Ref.. #2.1.3.3)** have assumed that overpressure in the Sable Subbasin is caused primarily by compaction disequilibrium and gas generation.

2.1.4 Reservoir Stratigraphy

Sable Offshore Energy Project gas reservoirs all occur stratigraphically within the Late Jurassic to Early Cretaceous Mic Mac and Missisauga formations. They consist of deltaic and shallow marine sands deposited within the Sable Delta complex. This delta complex was sourced from the north and prograded southward through time. The maximum southward extent was at the very top of the Missisauga Formation immediately below the capping Naskapi Shale. Over the course of approximately 50 million years, the active portion of the Sable Delta complex advanced and retreated repeatedly in a general north-south direction as a result of fluctuations in sediment supply and relative sea level. Its deposits have a maximum thickness of 2500 metres in the Venture/Thebaud area, and consist of stacked, successive, coarsening-upward deltaic depositional cycles.

Gas is trapped only where there is a favourable combination of structure and seal lithology (shales). The sand/shale ratio is optimal for trapping gas toward the seaward margin of the delta complex, where there is significant interfingering of deltaic sandstones with pro-delta/marine shales. The southward progradation of the Sable Delta complex through time, and the associated upward increase in sand/shale ratio, account for the stratigraphic variation in reservoir levels in the **Sable Offshore Energy Project** fields. The more northern fields (Thebaud, Venture and South Venture) contain gas reserves in sandstones which are marginal to the delta complex; these occur stratigraphically in the Mic Mac and lower Missisauga Formation. The later arrival of deltaic sandstones at the more southern Project fields (North Triumph, Glenelg and Alma) provided favourable gas trapping conditions at the very top of the Missisauga Formation. **Figure 2.1.4.1** is a diagrammatic north-south cross-section of the Missisauga Formation showing the relative stratigraphic position of reserves in the Project fields.

The stratigraphy of the reservoir interval in the Venture, South Venture and Thebaud fields is broadly correlative. The North Triumph, Glenelg and Alma reservoirs are also broadly correlative, but are considerably younger than, and do not correlate with, the northern fields. Syndepositional growth faulting localized individual sand body distribution; this complicates high order correlation between fields located in different growth fault blocks. As a result, a unified sand nomenclature for the Project fields is not possible, and each field has its own internal sand nomenclature.

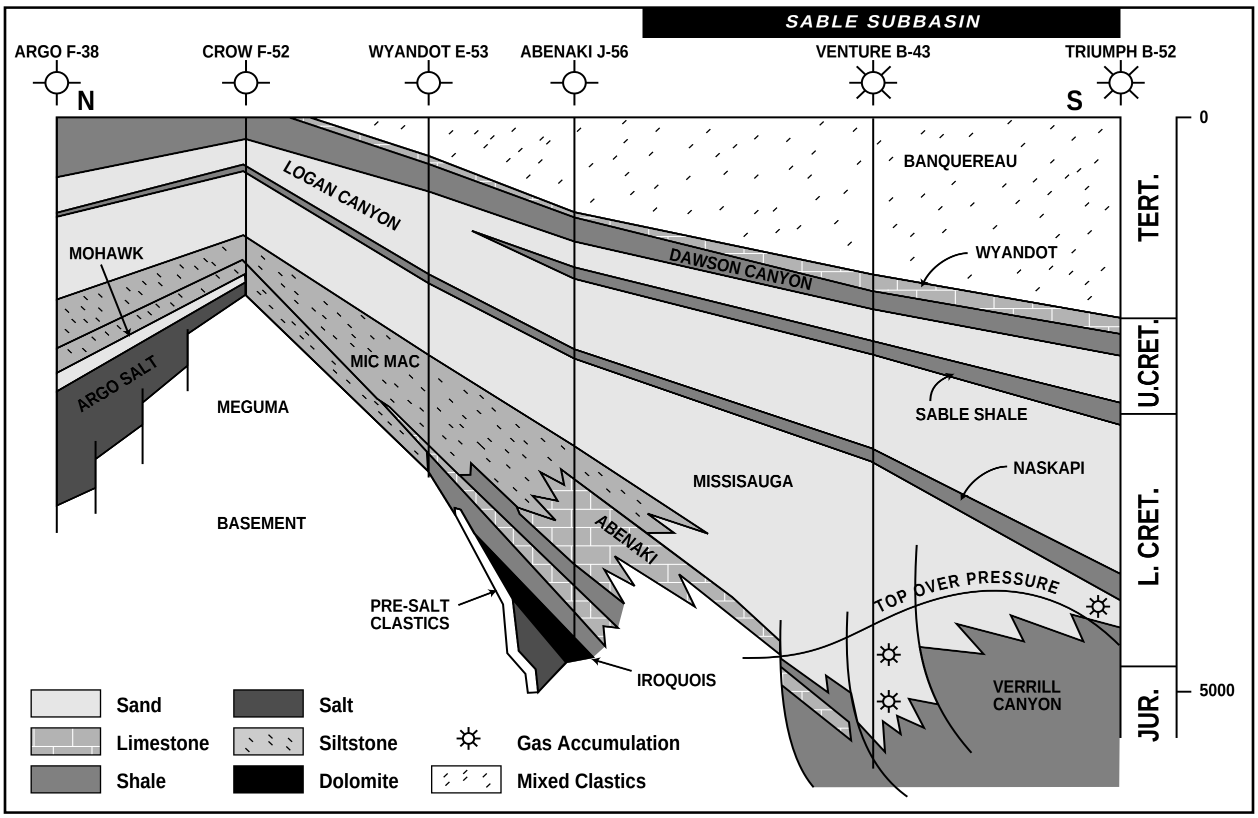

Modified after DPA Part 2 Ref# 2.1.2.2.

Figure 2.1.4.1 Diagrammatic North-South Cross-section of Missisauga Formation Showing Relative Stratigraphic Position of Gas Reserves in Project Fields.

2.1.5 Reservoir Sedimentology

Delta progradational shale to sand cycles 10 to 50 metres thick comprise the fundamental reservoir flow layers. **Figure 2.1.5.1** is a stratigraphic log from West Venture N-91 illustrating typical stacking of shale to sandstone coarsening-up cycles. This stacking resulted from repeated delta progradation and lobe switching.

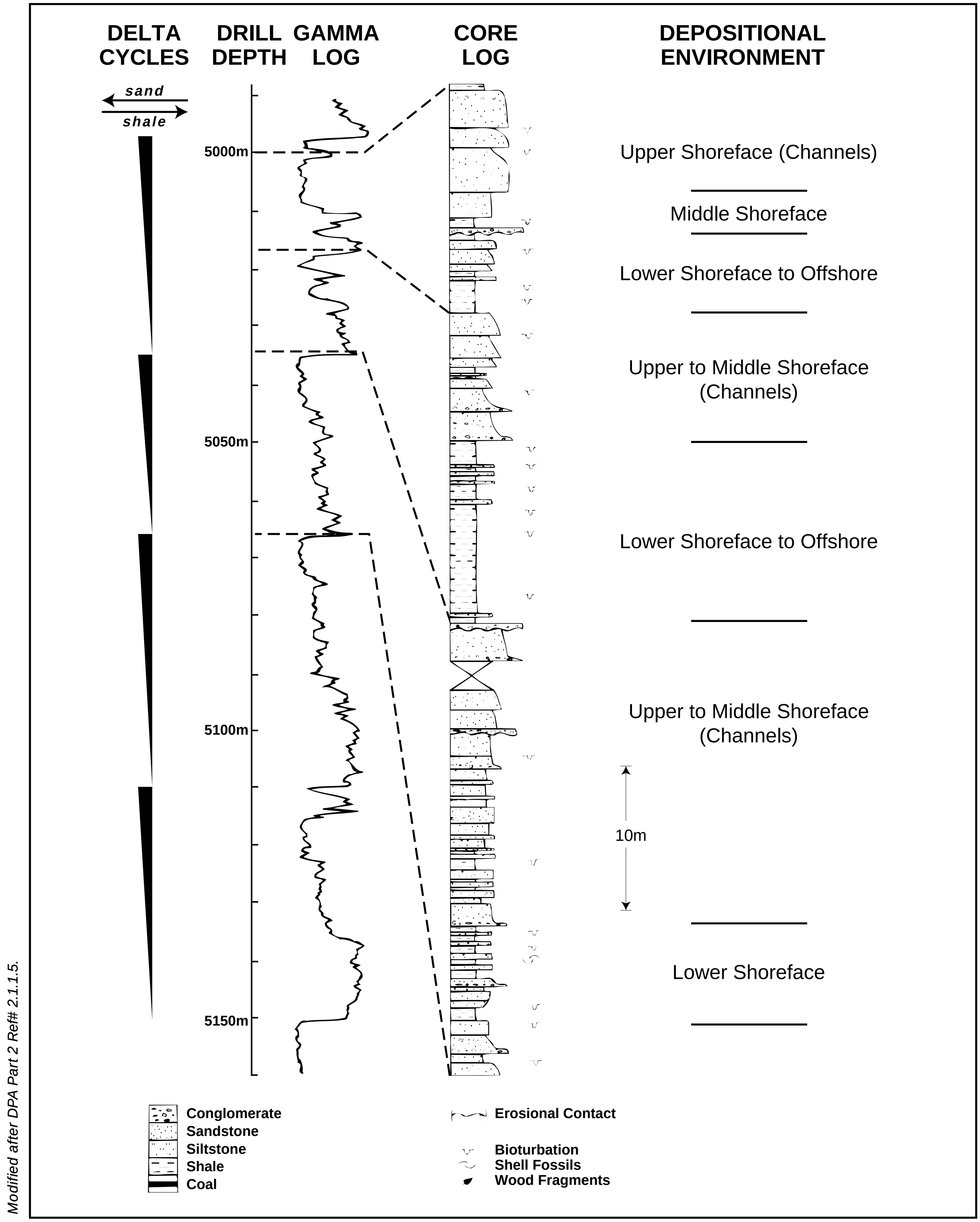

Figure 2.1.5.1: Stratigraphic Log showing stacked delta cycles.

The reservoir sands at the tops of these cycles belong to three depositional facies associations (**DPA - Part 2 Ref. # 2.1.5.1**). They are recognized based on lithology, sedimentary structures and lateral/vertical relationships. The Delta Plain Facies Association and Shelf and Strand Plain Facies Association are interpreted to have been deposited in a mixed-energy (predominantly tidal and wave dominated, but locally fluvially dominated) deltaic system. Sediments that comprise the Valley Fill Facies Association are interpreted as having been deposited within valley systems carved by distributaries into the underlying delta sediments at times of lowered relative sealevel. Sediments within these lowstand valley systems were deposited predominantly under tide-dominated estuarine conditions. **Figure 2.1.5.2** shows idealized vertical successions of the three depositional facies associations.

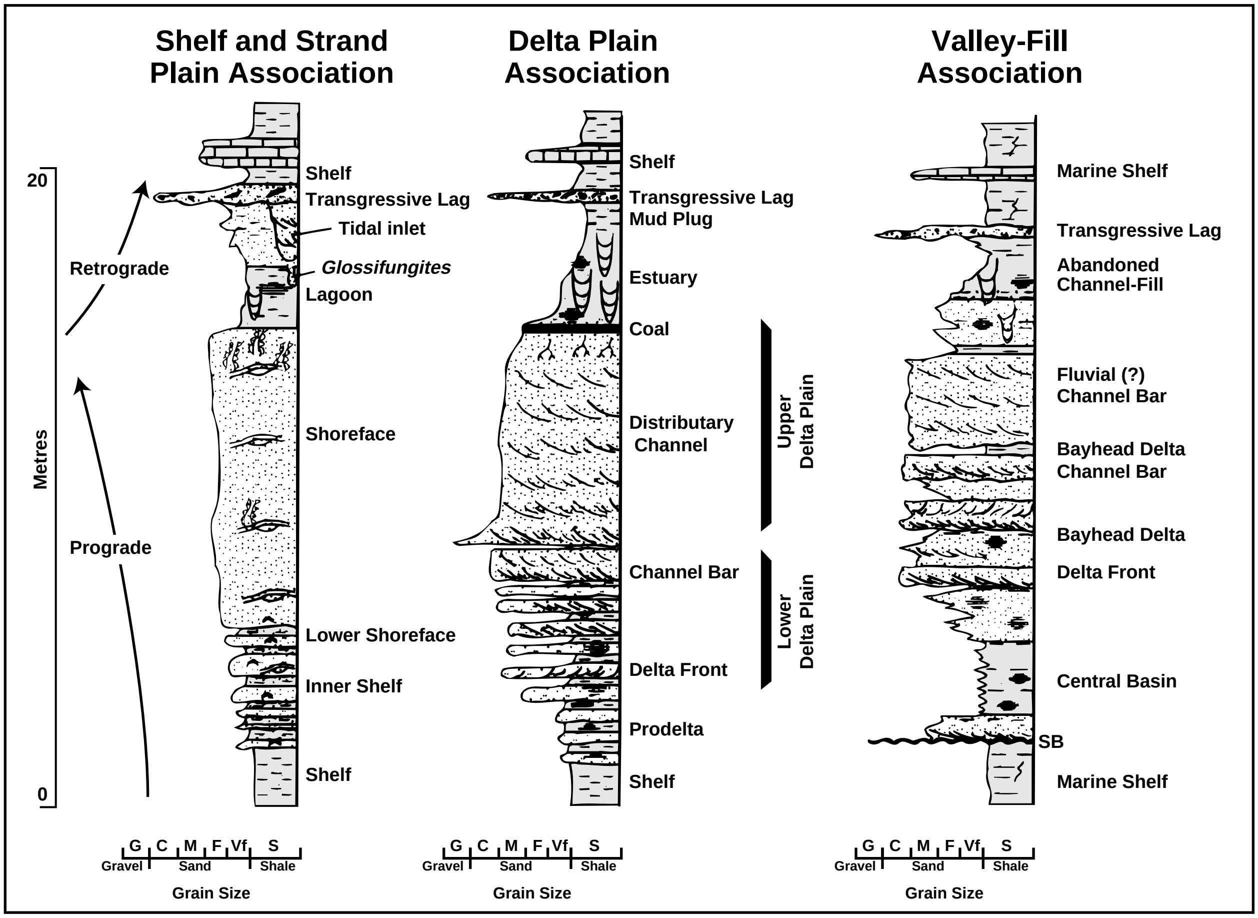

Figure 2.1.5.2: Facies Model, Sable Delta.

2.1.6 Reservoir Geophysics

Over 300,000 kilometres of 2D (two dimensional) seismic data has been acquired in the Scotian Shelf and slope since 1960; more than half of this since 1979 (**DPA - Part 2, Ref. #2.1.1.1**). The highest density of seismic data is located in the vicinity of Sable Island. Seismic acquisition geometry associated with the Project fields has been restricted to a single source and streamer configuration with limited shallow water or transition zone seismic over the western flank of the Venture structure.

Geophysical interpretations were carried out on all six fields during the mid to late 1980's. A variety of paper and workstation based approaches were used on the predominantly 2-D seismic database. Of the six fields, only Glenelg has conventional 3D (three dimensional) seismic coverage. A 1991 remapping of North Triumph incorporated a reconnaissance 3D seismic survey (focussed on the Chebucto structure) that largely covers the field.

Six regional markers; the Wyandot, Petrel, O Marker, Baccaro, Misaine and Scatarie; provide good mappable reflections throughout most of the subbasin. They have been used to define the regional setting for much of the Cretaceous and Upper Jurassic section. Numerous mappable events within the productive section of the northern fields (Venture, Thebaud and South Venture) are often limestones encased within sandstone/shale sequences or porous sands overlying tighter sandstones and shales. In the southern fields (North Triumph, Glenelg and Alma), mappable events are most often associated with the base of shale units. In both the northern and the southern fields, the mappable seismic events within the reservoir interval are often restricted areally to a single growth fault block.

Formation	Primary Seismic Reflectors	Dominant Lithology	Maximum Thickness
Sable Island		Sand and Gravel	
La Have		Clay	
Sambro		Sand	
Emerald		Silt	
Scotian Shelf		Glacial Drift	
Banquereau		Mudstone	1200 m
Wyandot	Wyandot	Chalk	230 m
Dawson Canyon	Petrel	Shale	900 m
Logan Canyon		Sandstone & Shale	250 m
		Shale	150 m
		Sandstone & Shale	600 m
Naskapi		Shale	230 m
Missisauga	"O" Marker	Sandstone	1130 m
Mic Mac		Calcareous Shale	1200 m
Verrill Canyon		Shale	>600 m
Abenaki	Baccaro	Limestone	750 m
	Misaine	Calcareous Shale	100 m
	Scatarie	Limestone	130 m
Mohawk		Sandstone & Shale	1070 m
Iroquois		Dolomite	200 m
Argo		Salt	>900 m

Modified from DPA Part 2 Ref# 2.1.1.1.

Figure 2.1.6.1: Primary Regional Seismic Reflectors, Scotian Basin

Synthetic seismograms (checkshot survey corrected), generated with all available wireline log sonic and density information from each field, were used to tie well lithology to the seismic data. The few vertical seismic profiles (VSPs) that have been acquired in the Project fields were also used to improve well data to seismic reflector ties.

The productive reservoirs in the northern fields are generally deeper than those in the southern fields and are predominantly overpressured. The overpressure does not appear to seriously degrade seismic quality and does not generate any discrete seismic events.

The velocity fields measured are generally well behaved and vary laterally in a slow and smooth manner. No significant velocity inversions are noted, although some velocity 'slowing' is observed within the overpressured section. Water depths range from surf zone on the western flank of Venture to a maximum of 90 metres over Glenelg. The water depths vary smoothly over the fields with little significant channeling. The overburden for these fields is typically flat lying with little structural disturbance.

Depth conversion of time structure maps for all six fields has been done using a vertical ray path or 'layer cake' technique. Methods applied to individual fields vary in degree of sophistication. These methods rely heavily upon well checkshot velocity information, and use some seismic stacking velocities to interpolate between, and extrapolate from, the well control where data quality permits. The resulting depth structure maps closely resemble the input time structure maps.

Reflection seismic has been used primarily to define the structural geometry of the fields, including fault plane geometry and reservoir juxtaposition. Some reservoir characterization based on amplitude mapping has been used in a limited way to guide appraisal drilling in the northern fields. The success of this technique has been restricted by the limited band width of the available seismic data.

A detailed analysis of several of the existing 2D datasets has indicated that modern 3D seismic has the potential to significantly improve the ability to map reservoir distribution and quality. Technical design work has been completed and preparation for the acquisition of 3D data, due to commence in 1996, is ongoing.

2.1.7 Reservoir Petrophysics

Full petrophysical evaluations have been completed on all six Project fields using a similar methodology. The details of the individual analyses vary according to the type and quality of the data available, and the vintage of the analysis. Listings of wireline log and core data are contained in the **CNSOPB** well history files for each well.

Reservoir sands are dominantly sublitharenites deposited as strand plain and channel sandstones. Their zonal average porosity and permeability range between eight and 20 percent, and one and 300 millidarcies (mD), respectively. The primary controls on porosity and permeability are average grain size, cementation and the presence of grain-rimming authigenic chlorite. Porosity tends to decrease with increasing depth, with the notable exception of clean overpressured reservoirs which have unusually high porosity. The occurrence of pervasive grain-coating chlorite in some overpressured reservoirs is believed to have inhibited the development of quartz cementation, preserving porosity at depth. Microporosity associated with the chlorite rims is also believed to result in locally high irreducible water saturation values. A broad range of average irreducible water saturation values, which vary from 10 to 40 percent, are calculated in the various reservoir sands of the **Sable Offshore Energy Project**.

Wherever possible, porosity was calculated from the density log measurement calibrated to stressed core porosity measurements. Porosity cutoff values between six and 10 percent were used in the determination of net porous sand thickness in the various reservoirs. These values were based on core and/or microlog indicated permeability, and correspond to permeability values between 0.1 and 1 mD to air at ambient conditions.

Water saturation values used in the estimation of gas in place were calculated using the Archie equation. Wherever possible, cementation and saturation exponent values were based on stressed core formation resistivity factor and resistivity index measurements. Formation water salinity values are high based upon the analyses of fluid recoveries from repeat formation test (RFT) and drillstem test (DST) fluid samples.

Typically, salinity increases with depth, reaching values as high as 100 to 300 thousand ppm sodium chloride. True formation resistivity was generally based on the deep induction measurement. In sands severely affected by drilling mud filtrate invasion, such as Venture, capillary pressure data was used extensively in the estimation of water saturation.

2.1.8 Gas in Place

Gas in place (GIP) estimates have been generated for all fields using both deterministic and probabilistic methods. The probabilistic estimates are considered to be the most representative, because they were generated using probability distributions for geological and petrophysical parameters that capture a range of uncertainty. Differences between the deterministic estimates and the P50 and mean values of the probabilistic estimates are due to the deterministic maps representing an unrisked gas accumulation. A description of the deterministic and probabilistic estimates for each field is outlined in the appropriate sections of this chapter.

Probabilistic gas in place determination was conducted in 1995 using Palisade @Risk™ software. This methodology permits recognition of uncertainties in the key input parameters. These parameters are: area, net pay development, porosity, water saturation, and expansion factor. Volume estimations are output as a range of possible values, with each value assigned a probability of occurring. The range of output values is dependent on the degree of uncertainty, or spread in range, of the input parameters. Future data acquisition and technical studies will be targeted to clarify these uncertainties. The results of the probabilistic analysis for the Project fields are shown in **Table 2.1.8.1**. This table expresses the gas in place estimate as the mean, or expected value, taken from the cumulative probability expectation curve. Gas in place at three other probability levels, P90, P50 and P10 are also presented. These values reflect possible gas in place volumes at different confidence levels. The total field P10, P50 and P90 gas-in-place numbers reported in Table 2.1.8.1 for SOEP fields consisting of a number of stacked pools (all but North Triumph) is an arithmetic summation of the reserves estimations at these confidence levels for each pool. For example, the P10 value shown for the Thebaud Field represents the arithmetic summation of all the P10 values for the constituent pools (see Table 2.2.1.7.1). This summation procedure was adopted for the sake of simplicity. Statistically the inference of this addition is of dependence between the stacked pools: the result is a wider range between the P10 and P90 reserves numbers for the fields than would result from a statistically independent summation. The degree of dependence between the stacked pools is not known, but likely varies in association with stratigraphic proximity, seal effectiveness, and fault juxtaposition.

Table 2.1.8.1: Probabilistic Gas In Place, E9M3

Field	P90	P50	P10	Mean
Thebaud	10.7	22.9	45.0	**26.0**
Venture	18.1	41.9	89.7	**49.2**
North Triumph	6.2	14.2	25.2	**15.2**
South Venture	3.4	10.4	20.5	**11.3**
Glenelg	7.1	12.1	17.9	**12.3**
Alma	11.5	14.9	18.7	**15.0**

2.1.9 Future Data Acquisition Strategy

During the pre-development and development phases of the Project, a data acquisition strategy will be initiated to refine current reservoir descriptions and narrow the uncertainty range associated with present gas in place estimates. This strategy includes the acquisition of 3D seismic data and the collection of wellbore data in development wells. The interpretation of these data will be used in the reservoir management of the Project fields such that recovery and value are optimized.

Future coring and logging programs will be designed to adequately evaluate development wells and clarify uncertainties unresolved by the present database. For example, core samples will be cut over selected intervals to augment the existing core database. A standard open-hole logging suite, including induction or laterolog resistivity, sonic, neutron and density tools, will be run over the reservoir section, wherever practical and safe to do so. However, formation imaging surveys and wireline formation tests may also be run, on occasion, to complement the standard open hole logging suite. Cased hole pulsed neutron logs and production logs will also be run, as required, to monitor reservoir performance.

This strategy begins with the acquisition of some 3D seismic data during the 1996 season. The interpretation of the seismic data will initiate remapping of Project fields and result in the complete integration of seismic data, most recent interpretations of existing well datasets, and current geologic models. Refinement of the map suite will continue, as stratigraphic and petrophysical relationships are further defined, based upon wireline log and core data obtained through development drilling.

2.2 Field Descriptions

This section presents a summary description of each field under the following subheadings: drilling history, reservoir description and zonation, geophysics, petrophysics, and gas in place assessments. Detailed information and the technical evaluations in support of these summaries are included in Part Two of this Development Plan Application.

The fields will be summarized in this section in the following order: Thebaud, Venture, North Triumph, South Venture, Glenelg, and Alma. **Table 2.2.1** presents a listing of basic well data for all wells drilled in the six **Sable Offshore Energy Project** fields.

Table 2.2.1: Well Data

Field	Number of Wells Drilled	Well I.D.	Year Drilled	Total Depth (metres)	Rotary Table (R.T.) to Sea Level (metres)	Water Depth (metres)
Thebaud	4	P-84	1972	4115	28.7	25.9
		I-94	1978	3962	29.9	28.0
		I-93	1985	5166	36.3	30.0
		C-74	1986	5150	41.8	31.0
Venture	5	D-23	1979	4945	31.7	20.1
		B-13	1981	5368	34.1	24.7
		B-43	1982	5872	34.1	20.4
		B-52	1983	5960	35.4	19.5
		H-22	1984	5944	38.4	22.0
North Triumph	2	G-43	1986	4504*	24.0	74.0
		B-52	1986	3960	24.0	81.0
South Venture	1	O-59	1983	6176	35.4	24.0
Glenelg	4	J-48	1983	5148	24.0	82.0
		E-58	1984	4154	24.0	79.0
	Whip	E-58a	1984	4192*	24.0	75.0
		H-38	1985	4865	24.0	88.0
		N-49	1986	4040	23.0	72.0
Alma	2	F-67	1984	5054	24.0	68.0
		K-85	1985	3602	24.0	68.0

* measured depth

2.2.1 THEBAUD FIELD

2.2.1.1 Field History

In 1972, the discovery well, P-84, encountered gas pay in several, vertically stacked, hydropressured and overpressured sandstone horizons. Three delineation wells, I-94, I-93 and C-74, were drilled in 1978, 1985 and 1986, respectively, to evaluate the structure. These delineation wells established that hydropressured gas accumulations encountered in P-84 were of limited areal extent. The first overpressured reservoir, the A Sand, was found to be entirely gas bearing in P-84 and in all three appraisal wells confirming the presence of a significant gas accumulation. The A Sand reservoir occurs at a depth of 3828 metres R.T. (Rotary Table) in the P-84 wellbore. The most recent delineation wells, I-93 and C-74, were drilled deeper into the overpressured section. The C-74 well successfully encountered several additional gas bearing overpressured sandstone horizons. The onset of overpressure in the Thebaud structure occurs at a depth of about 3800 metres. **Figure 2.2.1.1.1** is a depth structure map of the top A Sand and shows the Thebaud Field well locations.

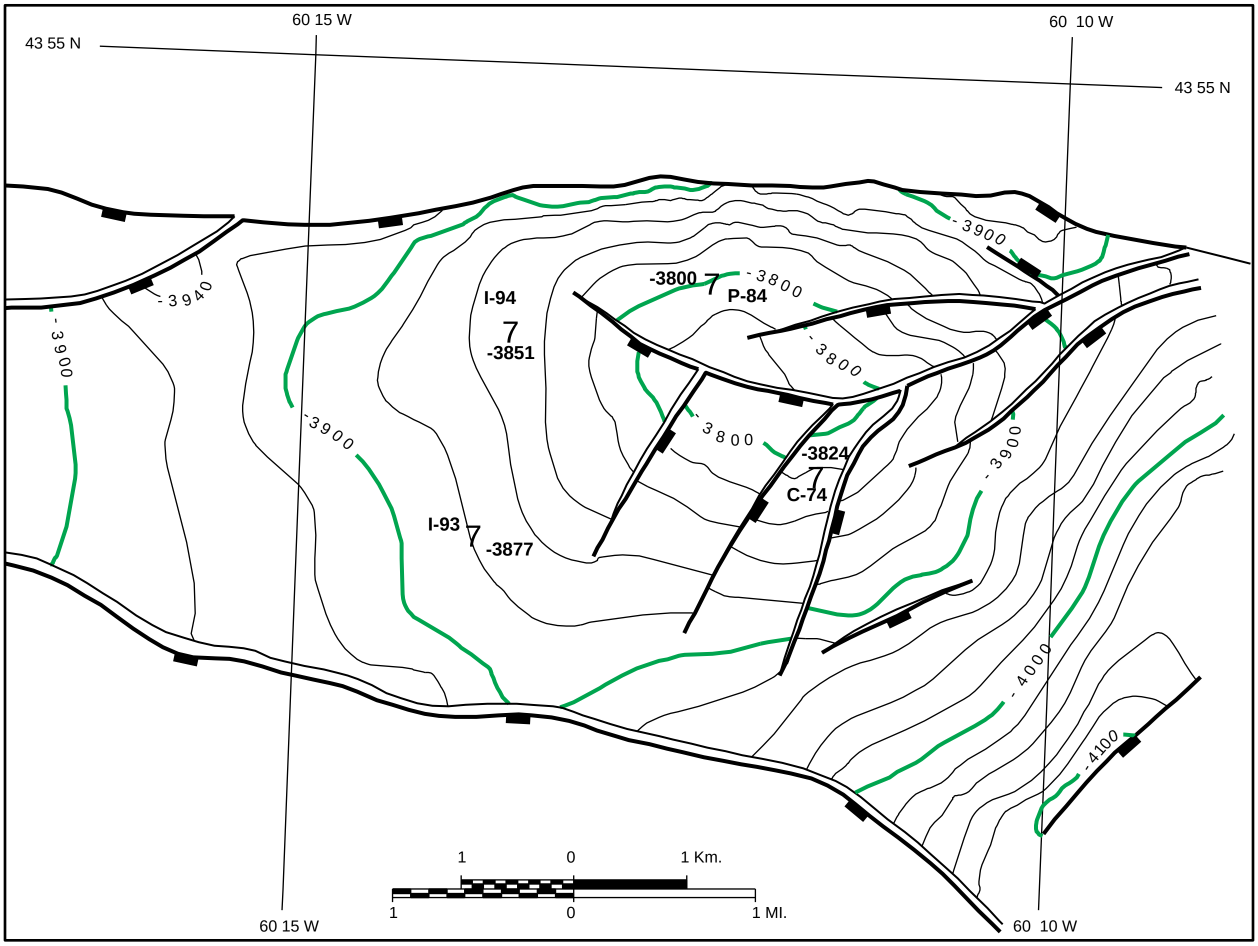

Figure 2.2.1.1.1 Thebaud Field - Top A Sand Depth Structure Map
Contour Interval: 20 Metres

2.2.1.2 Structural Configuration

The Thebaud structure is a rollover anticline on the downthrown side of a major down to the basin growth fault. At the A Sand horizon, the anticline is approximately six kilometres by five kilometres in size and encompasses an area of 31.6 square kilometres with a vertical closure of 160 metres. Gross closure at the A Sand level is established by a saddle spillpoint located on the western side of the structure. Several minor faults that occur within the structure are discontinuous at this horizon. These faults generally have displacements less than the A Sand thickness, and result in sand-to-sand juxtaposition within the structure.

2.2.1.3 Geology

The Thebaud Field is located along an east-west trend of growth fault related structures. The reservoir section in Thebaud is Late Jurassic and Early Cretaceous, Mic Mac and lower Missisauga formations. A considerable thickness of deltaic clastics is preserved within the Thebaud structure. The productive interval encountered extends from 3200 metres to 4930 metres, a gross thickness of 1730 metres.

Gas accumulations are identified within hydropressured and overpressured reservoir sandstones. They occur within a vertically stacked, alternating sequence of sandstones, shales and occasional limestones. This repetitive cyclic sedimentation is the result of episodic delta progradation that is punctuated by periods of marine incursion associated with relative sea level change. Individual delta progradations are characterized on wireline logs by 20 to 35 metre thick, coarsening, cleaning upward packages. Reservoir quality sandstones occur within the upper portion of these delta progradations. Overlying shales, associated with marine flooding surfaces, are interpreted to be areally extensive, and provide the top seal to individual gas accumulations.

Gas has been tested in four independent hydropressured reservoir horizons in the P-84 discovery well. Subsequent delineation wells were drilled structurally downdip from this location. Log analysis in I-93, the structurally lowest well, indicated all equivalent sands to be wet or tight. Log analysis in I-94 and C-74 interpreted minor gas pay thicknesses above water in these sands. Gas accumulations in the hydropressured section are of limited areal extent around the crestal P-84 well.

The A Sand is the first overpressured reservoir encountered in the Thebaud structure and has been penetrated and tested in all four wells. Wellbore net pay thickness for the A Sand horizon varies from 14 metres in the I-93 well, to 26 metres in the I-94 well. Wellbore and seismic data indicate that A Sand gross thickness decreases from north to south, away from the north bounding fault. This observation is consistent with the geologic model, where reservoir sandstones are interpreted to thicken toward the master growth fault. Gas is trapped at the A Sand level by a combination of simple rollover closure, and fault closure to the north by juxtaposition against an interpreted shale rich lithology. **Figure 2.2.1.3.1** is a net pay thickness map of the A Sand reservoir.

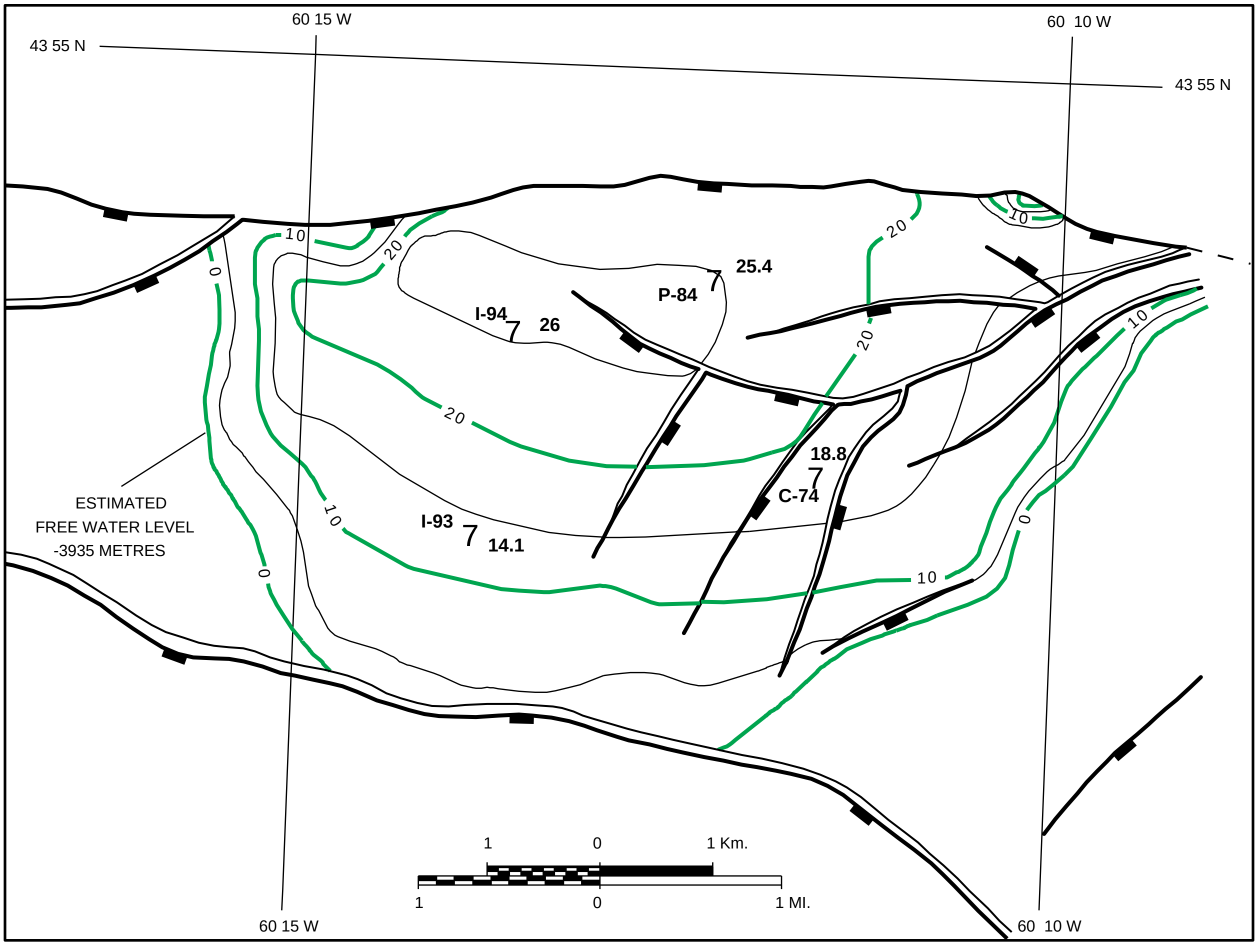

Figure 2.2.1.3.1 Thebaud Field - Sand A Net Pay Thickness Map
Contour Interval: 5 metres

The C-74 well tested high gas flowrates from a number of deeper, overpressured sandstones. Equivalent sandstones at a structurally downdip location in the I-93 well, are generally of poorer reservoir quality. Stratigraphic correlation between these two wells in the deep section, however, is problematic. The deeper overpressured section encountered in the I-93 well is characterized by a lower overall sand-to-shale ratio.

2.2.1.4 Reservoir Zonation

The stratigraphic nomenclature used for the Thebaud Field reservoir section is illustrated in **Figure 2.2.1.4.1**, a schematic cross-section incorporating the I-93 and C-74 wells. Wireline log response, core, pressure, and seismic data were used to subdivide the Thebaud reservoir section into this series of reservoir sandstone packages. Sandstone reservoirs that have flowed gas on drillstem test are depicted on the schematic cross-section. The overpressured G2 horizon was not tested, but is included due to favourable log interpretation in the C-74 well and proximity to the tested G3 Sandstone. The alpha numeric nomenclature assigned to these reservoir sandstones is unique to the Thebaud structure and is not applied to other Project fields. Uncertainty exists in the correlation of the deeper overpressured sandstone reservoirs. This is due to a general deterioration in the quality of seismic data and greater intrafield fault complexity. The deep overpressured section in I-93 has been interpreted in deterministic reservoir studies to represent a more distal fine grained delta facies. However, improved seismic data is needed to resolve the relationship between intrafield faults and reservoir stratigraphy in this deep section.

The A Sand is the largest single reservoir accumulation identified to date in the Thebaud structure. Consequently, deterministic reservoir studies conducted in the 1980's further subdivided the A Sand into four reservoir rock type layers for input to reservoir simulation models (**DPA - Part 2, Ref. 2.1.4.1**). These rock types were determined from core and log sedimentary and reservoir facies analysis. All other reservoir sandstones were mapped as single layers for purposes of gas in place estimation and reservoir simulation input.

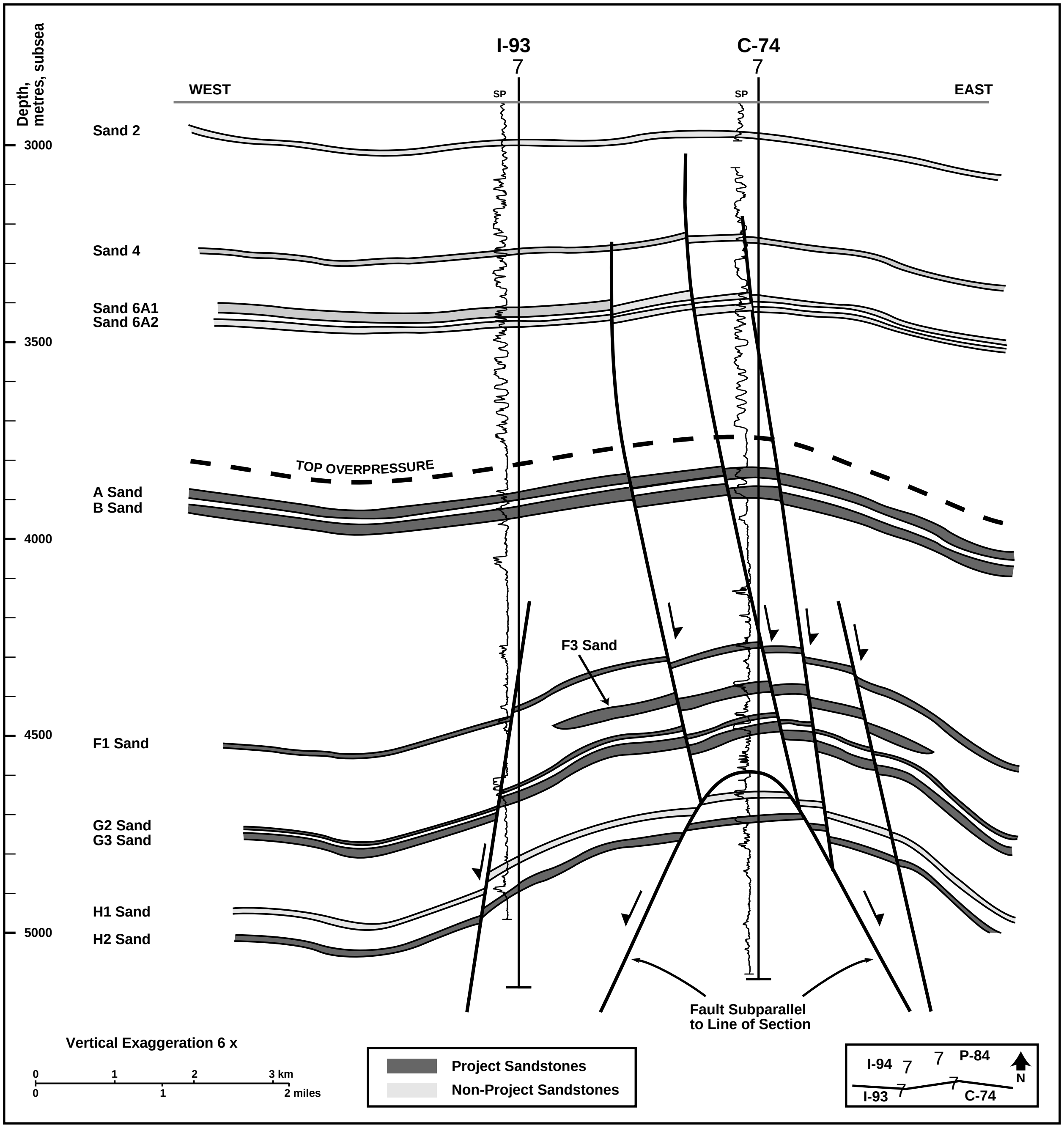

Figure 2.2.1.4.1: Thebaud Schematic Structural Cross-section

2.2.1.5 Geophysics

2.2.1.5.1 Seismic Database

Six 2D seismic datasets have been acquired over the Thebaud structure since the early 1980s. All datasets share similar characteristics. A summary of acquisition and processing details for several of these datasets is included in **Table 2.2.1.5.1.1**.

The seismic data density and quality at the main project reservoir A Sand is quite good. When incorporated with the well data, a moderately high level of confidence is generated at the A Sand level. Continuity, frequency content, and fault imagery, however, deteriorate at greater depths. This results in a considerable decrease of confidence in the deeper maps. Analysis of the seismic data indicates that significant, broadband signal is present in the seismic data at depth. The same analysis shows that overpressure has only a minor effect on sonic velocities and imaging. The poor quality of the deeper seismic is thought to be largely a function of 2D crossline dip. The acquisition parameters used, and the processing stream applied in an operationally challenging environment, have also reduced the quality of the deeper seismic. The depth structure maps used for gas in place estimates are based on the 2D seismic data grid illustrated in **Figure 2.2.1.5.1.1.**

Table 2.2.1.5.1.1: Thebaud Acquisition and Processing Summary

Data Type	Survey Name	Incorp. In Study	Acq. Date	Acq. Style	Proc. Date	Field Kms	Proc. Details	Comments
2D	8624-M003-047E	Yes	1984	Marine	1984-85	359	60 fold Decon before and after stack, FD migration	Good to very good data quality, poorer with depth, lower frequency
2D	90-1200's	No	1990	Marine	1990-91	18	60 fold Decon before and after stack, FD migration	Good to very good data quality, better fault definition and frequency
2D	91-1400's	No	1991	Marine	1991-92	81	60 fold Decon before and after stack, Kirchoff migration	Good to very good data quality, better fault definition and frequency
2D	8620-S014-006E	No	1983	Marine	1983-84	84	60 fold Desig, Decon after stack, FD migration	Generally fair to good data quality
2D	8624-M003-044E	No	1982	Marine	1982-83	8	60 fold Desig, Decon after stack, F-K migration	Generally good data quality
2D	8620-M003-033E	No	1979	Marine	1979-80	82	60 fold Decon before and after stack, FD migration	Generally fair to good data quality

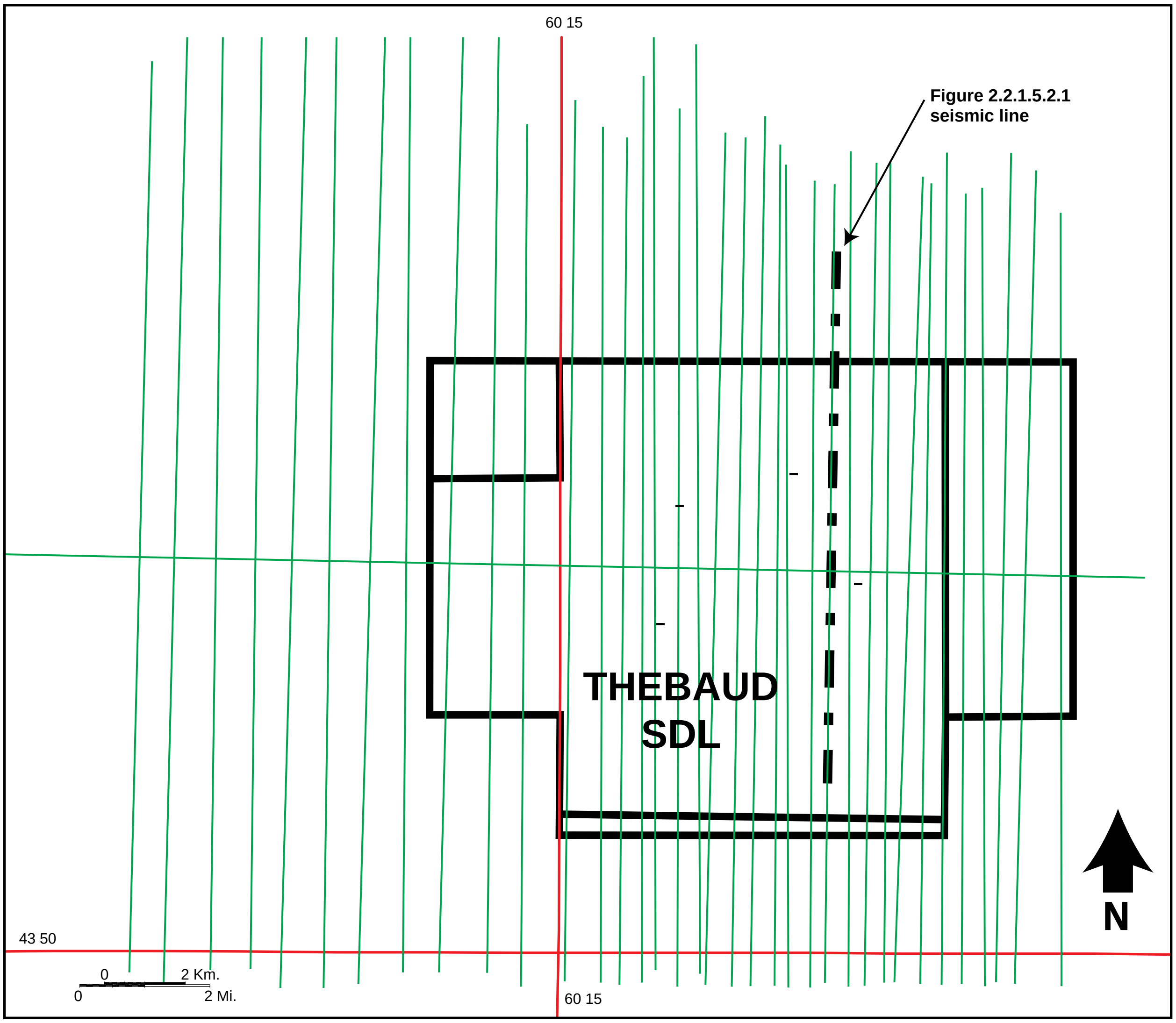

Figure 2.2.1.5.1.1: Thebaud Seismic Database Map

2.2.1.5.2 Time Interpretation

The maps used for gas in place (GIP) calculations at Thebaud are based on time and depth structure maps made in 1987. This interpretation was generated on a Landmark™ workstation using the 1984 dataset exclusively. The 1984 survey consists of 33 dip lines and one strike line for a total length of 359 line kilometres. The strike line runs 12.5 kilometres from east to west across the southern flank of the structure at the A Sand level. The dip lines have an east to west line spacing of approximately 300 metres over the crest and flanks of the structure.

Checkshot survey corrected synthetic seismograms, generated at each well by convolving a minimum phase wavelet with an acoustic impedance series derived from wireline log sonic and density information, were used to tie well lithology to the seismic data. The C-74 VSP was also used to improve the well data to seismic reflector tie.

A large number of horizons were interpreted on the workstation. The O Limestone Marker, 5A Sand, B Sand, F1 Sand and G2 Sand horizons were taken to final mapped form and used as the basis for the depth structure maps. **Table 2.2.1.5.2.1** lists the horizon markers at each of the four Thebaud wells.

Table 2.2.1.5.2.1: Thebaud Horizon Markers

	P-84		I-94		I-93		C-74	
MAP HORIZON	Depth (M, ss)	TWT (sec)	Depth (M, ss)	TWT (sec)	Depth (M, ss)	TWT (sec)	Depth (M, ss)	TWT (sec)
ZONE 1	-2582.2	2118	-2602.1	2142	-2615.0	2152	-2605.2	2164
O MARKER	-2887.3	2273	-2932.5	2303	-2961.0	2329	-2945.9	2328
ZONE #5A	-3236.0	2436	-3293.0	2468	-3316.5	2494	-3289.7	2495
B SAND	-3846.8	2745	-3894.7	2765	-3913.0	2784	-3862.6	2762
F1 MARKER	NDE	NDE	NDE	NDE	-4415.2	3032	-4264.7	2967
G2 MARKER	NDE	NDE	NDE	NDE	-4600.7	3129	-4436.5	3067

NDE - Not Deep Enough

The time structure maps are included in Part Two of this document (**DPA - Part 2, Ref. # 2.2.1.5.2.1**). Geophysical modeling and amplitude work was done to aid in positioning the C-74 well at the A Sand interval. Although these techniques are restricted by the limited bandwidth and data quality of the 1984 dataset, the post-drill results compared favourably with the pre-drill estimate. A seismic line representative of the data quality and illustrating the field geometry is shown in **Figure 2.2.1.5.2.1** and is identified with a bold dashed line in **Figure 2.2.1.5.1.1.**

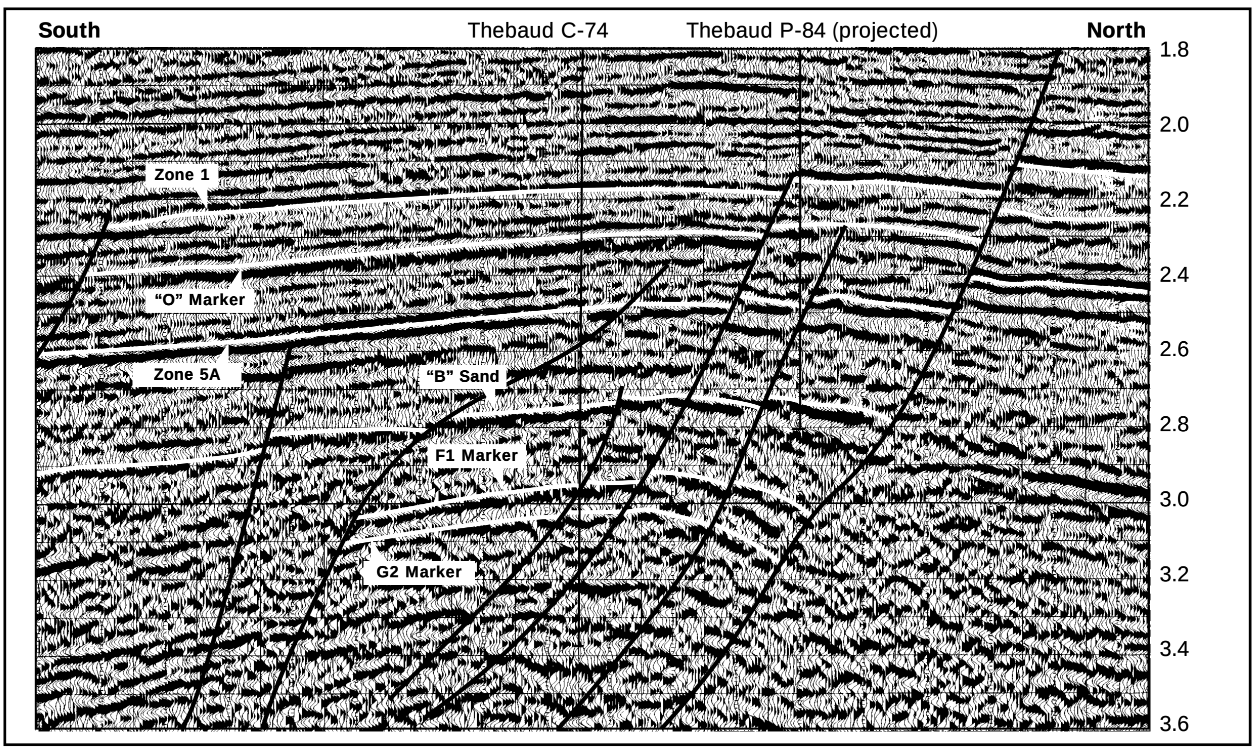

Figure 2.2.1.5.2.1: Thebaud Seismic Line

In 1990 and 1991, approximately 1400 kilometres of 2D data were acquired over the Thebaud Field and surrounding acreage. These data sets showed improvement in frequency content and resolution at the A Sand interval, and began to capture fault image energy. As with the 1984 dataset, the data deteriorated below the A Sand interval. Neither of these datasets have been used to update the current mapping suite.

2.2.1.5.3 Depth Conversion

Velocity surveys from each of the four Thebaud wells (**Table 2.2.1.5.3.1**) were used to generate average velocity values to each of the mapped horizons.

Table 2.2.1.5.3.1: Thebaud Velocity Surveys

Well	Year Acquired	Checkshot Available	Checkshot Type	VSP Available	VSP Type
Thebaud P-84	1972	Yes	Vertical	No	NA
Thebaud I-94	1978	Yes	Vertical	No	NA
Thebaud I-93	1985	Yes	Vertical	No	NA
Thebaud C-74	1986	Yes	Vertical	Yes	Vertical

These discrete values were hand contoured for each horizon following trends extracted from the 1984 2D seismic stacking velocity data. Seismic lag maps were generated for each time mapped horizon using values calculated at every well and were used to lag correct each of the time structure maps. The gridded average velocity maps and the gridded corrected time structure maps were combined to create the depth structure maps. Depth maps on intermediate horizons were generated from hand contoured wellbore thickness data. The velocity and final depth maps are included in Part Two of this document (**DPA - Part 2, Ref. # 2.2.1.5.3.1**).

2.2.1.6 Petrophysics

A detailed petrophysical evaluation of all four wells in the Thebaud Field was conducted using all available wireline log data, conventional/special core analysis data (**DPA - Part 2, Ref. # 2.2.1.6.1**), and pressure data. A detailed summary of the interpretation parameters and methodology is included in this document (**DPA - Part 2 Ref. # 2.2.1.6.2**). The results of this evaluation are illustrated in **Tables 2.2.1.6.1** to **2.2.1.6.4**.

Table 2.2.1.6.1: Thebaud P-84 Project Reservoir Parameter Summary

Sand Unit	Measured Depth Top (m)	Measured Depth Base (m)	Elevation Top (m ss)	Elevation Base (m ss)	Gross Thickness (m)	Net Pay (m)	Average Porosity (%)	Average Sw (%)	Average Permeability* (mD)
A	3828.3	3855.0	-3799.6	-3826.3	26.7	25.4	18.3	29.3	82.4
B	3875.5	3920.0	-3846.8	-3891.3	44.5	15.1	10.5	60.0	4.5
F1	NDE	-	-	-	-	-	-	-	-
F3	NDE	-	-	-	-	-	-	-	-
G2	NDE	-	-	-	-	-	-	-	-
G3	NDE	-	-	-	-	-	-	-	-
H2	NDE	-	-	-	-	-	-	-	-

NDE - Not Deep Enough

* based on core analysis porosity vs permeability transforms

Table 2.2.1.6.2: Thebaud I-94 Project Reservoir Parameter Summary

Sand Unit	Measured Depth Top (m)	Measured Depth Base (m)	Elevation Top (m ss)	Elevation Base (m ss)	Gross Thickness (m)	Net Pay (m)	Average Porosity (%)	Average Sw (%)	Average Permeability* (mD)
A	3880.7	3912.0	-3850.8	-3882.1	31.2	26.0	19.5	42.5	76.1
B	3924.6	NDE	-3894.7	NDE	22.4 (min)	0.0	-	-	-
F1	NDE	-	-	-	-	-	-	-	-
F3	NDE	-	-	-	-	-	-	-	-
G2	NDE	-	-	-	-	-	-	-	-
G3	NDE	-	-	-	-	-	-	-	-
H2	NDE	-	-	-	-	-	-	-	-

NDE - Not Deep Enough

* based on core analysis porosity vs permeability transforms

Table 2.2.1.6.3: Thebaud I-93 Project Reservoir Parameter Summary

Sand Unit	Measured Depth Top (m)	Measured Depth Base (m)	Elevation Top (m ss)	Elevation Base (m ss)	Gross Thickness (m)	Net Pay (m)	Average Porosity (%)	Average Sw (%)	Average Permeability* (mD)
A	3912.8	3932.5	-3876.5	-3896.2	19.7	14.0	16.4	51.1	44.4
B	3949.3	3981.0	-3913.0	-3944.7	31.7	0.0	-	-	-
F1	4451.5	4461.2	-4415.2	-4424.9	9.7	0.0	-	-	-
F3	-	-	-	-	-	-	-	-	-
G2	4637.0	4644.6	-4600.7	-4608.3	7.6	0.0	-	-	-
G3	4652.0	4677.3	-4615.7	-4641.0	25.3	5.9	10.9	65.0	-
H2	4915.3	4929.5	-4879.0	-4893.2	14.2	9.1	9.8	54.0	-

* based on core analysis porosity vs permeability transforms

Table 2.2.1.6.4: Thebaud C-74 Project Reservoir Parameter Summary

Sand Unit	Measured Depth Top (m)	Measured Depth Base (m)	Elevation Top (m ss)	Elevation Base (m ss)	Gross Thickness (m)	Net Pay (m)	Average Porosity (%)	Average Sw (%)	Average Permeability* (mD)
A	3865.6	3888.1	-3823.8	-3846.3	22.6	18.8	17.8	49.9	36.3
B	3904.4	3943.4	-3862.6	-3901.6	39.0	25.2	15.4	45.0	112.5
F1	4306.5	4320.2	-4264.7	-4278.4	13.7	6.1	12.8	43.0	-
F3	4405.2	4427.7	-4363.4	-4385.9	22.5	15.2	18.8	19.0	-
G2	4478.3	4486.7	-4436.5	-4444.9	8.4	7.0	16.9	27.0	-
G3	4506.0	4523.0	-4464.2	-4481.2	17.0	12.3	17.0	33.0	-
H2	4747.0	4762.0	-4705.2	-4720.2	15.0	10.3	13.3	22.0	-

* based on core analysis porosity vs permeability transforms

Zonal average porosity ranges from 10 to 23 percent. The primary controls on porosity and permeability are average grain size, cementation and the presence of grain-rimming authigenic chlorite which preserves intergranular porosity. Porosity preservation in clean sands of the overpressured section is generally associated with the pervasive occurrence of grain-coating chlorite rims which inhibited the development of pore filling quartz overgrowths. High irreducible water saturations, believed to be related to the presence of grain-rimming authigenic chlorite, are observed in some horizons.

Porosity was calculated from both density and sonic log measurements. Bulk density calibrated to stressed core porosity measurements was the preferred method. Where the density log measurements were of poor quality, due to hole washout or gas effects, sonic log porosity was used. Both density and sonic log porosity calculations were corrected for shaliness, and where necessary the sonic log was corrected for gas effect.

The Archie equation was used to determine water saturations in all the reservoirs. The cementation and saturation exponent values were based on special core analysis and log data crossplots. True formation resistivity was determined from the deep induction measurement corrected for borehole effects and invasion. Formation water resistivity was based on a formation water salinity gradient determined from drillstem test recoveries, and formation temperature gradients.

An in situ porosity cutoff value of 8 percent was generally used to define net porous sand thickness. In some sands cutoff values between 6 and 14 percent were used, based on core and microlog data. These values were all determined from core data to correspond to an air permeability value of 0.1 mD at ambient conditions. A water saturation cutoff of 70 percent was used to define net pay.

In only a few cases do existing wells intersect the gas/water contact. Therefore, free water level estimates were based on bracketing of the contacts from wireline log analysis and drillstem test results, and capillary pressure measurements.

2.2.1.7 Gas In Place

Gas in place estimates for the Thebaud Field have been generated using deterministic and probabilistic methods. The probabilistic assessment of gas in place was conducted in 1995 and is described in **DPA - Part 2, Ref. # 2.2.1.7.1**. The summation of mean values from the output expectation curves generated for the seven Project sands is 26.0 E9M3. Results of the probabilistic assessment for each of the Project sands are shown in **Table 2.2.1.7.1**.

Table 2.2.1.7.1: Thebaud Probabilistic Estimates of Gas In Place, E9M3

Reservoir Sandstone	P90	P50	P10	Mean
A	6.3	11.9	20.6	**12.8**
B	0.7	1.6	3.3	**1.8**
F1	0.3	0.9	2.2	**1.1**
F3	1.1	2.7	6.0	**3.2**
G2	0.5	1.2	2.8	**1.5**
G3	1.0	2.3	5.3	**2.9**
H2	0.8	2.3	4.8	**2.7**
Project Total	10.7	22.9	45.0	**26.0**

Deterministic reservoir maps of the Thebaud Field were generated in 1987 and 1988. Gas in place estimates for Project sands shown in **Table 2.2.1.7.2** represent the unrisked volumes which include upside. The methodology and maps used to generate the deterministic gas in place estimates are contained in Part Two of this document (**DPA - Part 2, Ref. # 2.2.1.7.2 and 2.1.4.1**).

Table 2.2.1.7.2: Thebaud Deterministic Estimates of Gas In Place, E9M3

Reservoir Sandstone	Gas in Place
A	15.6
B	2.3
F1	0.7
F3	5.4
G2	2.9
G3	5.6
H2	7.1
Total	39.6

Some minor gas accumulations have been tested in Thebaud that are currently not included in the Project. Predominantly, these are hydropressured gas accumulations with probabilistic mean gas in place estimates between 0.1 and 0.3 E9M3.

2.2.2 VENTURE FIELD

2.2.2.1 Field History

In 1979, the discovery well, D-23, was drilled on the crest of the Venture structure. Gas was encountered in multiple, stacked, hydropressured and overpressured sandstone horizons. Top overpressure occurs at about 4500 metres in the Venture structure. Four delineation wells were subsequently drilled, B-13 (1981), B-43 (1982), B-52 (1983), and H-22 (1984). **Figure 2.2.2.1.1** illustrates the location of these wells on a depth structure map on the top Sand 6 reservoir horizon.

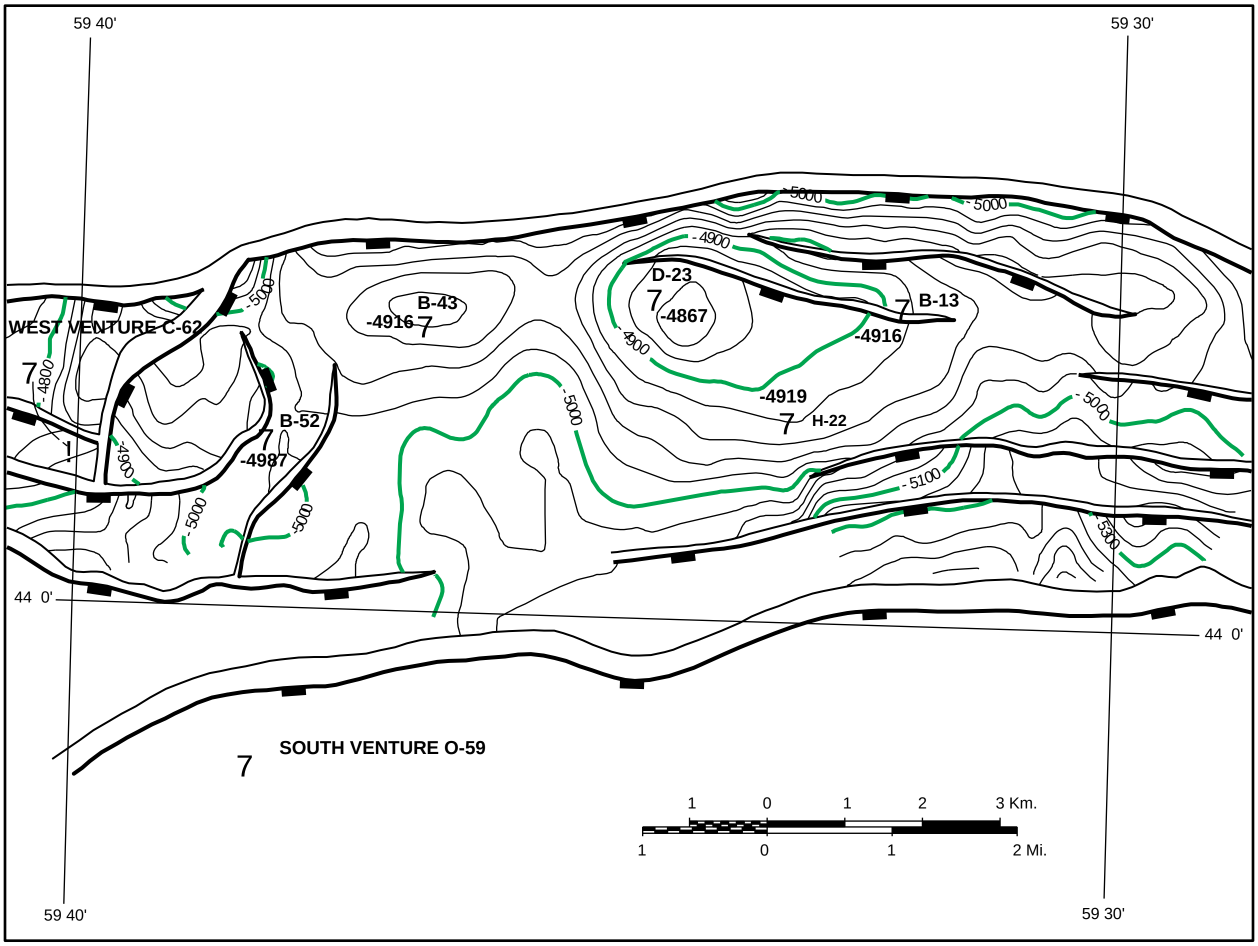

Figure 2.2.2.1.1: Venture Field - Top Sand 6 Depth Structure Map
Contour Interval: 20 metres

All four delineation wells were drilled deeper than the D-23 discovery, and encountered additional over-pressured gas accumulations. The B-13, B-52, and H-22 wells, drilled structurally downdip of the discovery well, tested water in several sandstone horizons and provided control for the areal extent of these accumulations. The B-43 well drilled on a structural high west of the discovery well, flowed gas in nine sandstone reservoirs. The H-22 well encountered tighter sandstones in the deep overpressured section and provided a southerly limit to reservoir development in these horizons. Results indicate that the majority of reservoir horizons are continuous and correlatable throughout all five wells.

2.2.2.2 Structural Configuration

The Venture structure is an elongated rollover anticline situated on the downthrown side of a listric, down to the basin, east-west trending growth fault. The anticline is approximately 12 kilometres long by three kilometres wide and encompasses an area of about 30 square kilometres. The structure is characterized by the occurrence of two structural crests and an intervening saddle. The western high is located near the existing B-43 well, and the eastern high is located near the D-23 well. Some discontinuous east-west trending faults with minor offsets are mapped within the field on the eastern structural high. These faults are synthetic to the northern bounding growth fault.

2.2.2.3 Geology

The reservoir section in Venture is late Jurassic and early Cretaceous in age and is situated stratigraphically within the Mic Mac and lower Missisauga formations. As in the Thebaud Field, an impressive thickness of deltaic clastics is preserved within the Venture structure. Gas accumulations occur within a stratigraphic interval of approximately 1780 metres, from 4045 to 5825 metres R.T. in the existing wells. The principal reservoir sandstones occur within a 695 metre interval from 4406 to 5101 metres R.T. The two uppermost reservoir horizons, Sands 1 and 2, are hydropressured. The remaining reservoir sands are overpressured.

Gas is trapped in sandstones that occur within a vertically stacked, alternating sequence of sandstones, shales and limestones. This cyclic pattern of sedimentation is interpreted to represent episodic delta progradations interrupted by marine floods. Shales and limestones deposited during the major marine floods form the top seals to individual reservoir accumulations. The Venture Field reservoir section is characterized by the occurrence of several substantial limestone horizons. These limestones are encountered in all the Venture Field wells and are demonstrated by seismic to be areally extensive.

Pressure versus depth plots (**DPA - Part 2, Ref. # 2.1.2.1**) show that abrupt, ‘step like’ pressure increases take place in the overpressured section. This results in a series of overpressured zones, each more overpressured than the zone above. Certain individual pressure steps are related to the presence of limestones and calcareous sandstones. Pressure correlation between wells indicates that overpressure steps are stratigraphically controlled. Correlative sands within the overpressured zone of the five wells have similar pressures.

Figure 2.2.2.3.1 is a net pay thickness map for the Sand 6 Upper reservoir. Net pay is assigned to four wells and varies in thickness from 10.1 metres in H-22 to 14.8 metres in B-43. The B-52 well is the structurally lowest well at this horizon and is entirely water bearing. An estimated free water level at 4970 metres subsea is derived from well pressure data. Gas is trapped at the 6 Upper level predominantly by rollover closure, and a 110 metre vertical gas column is interpreted.

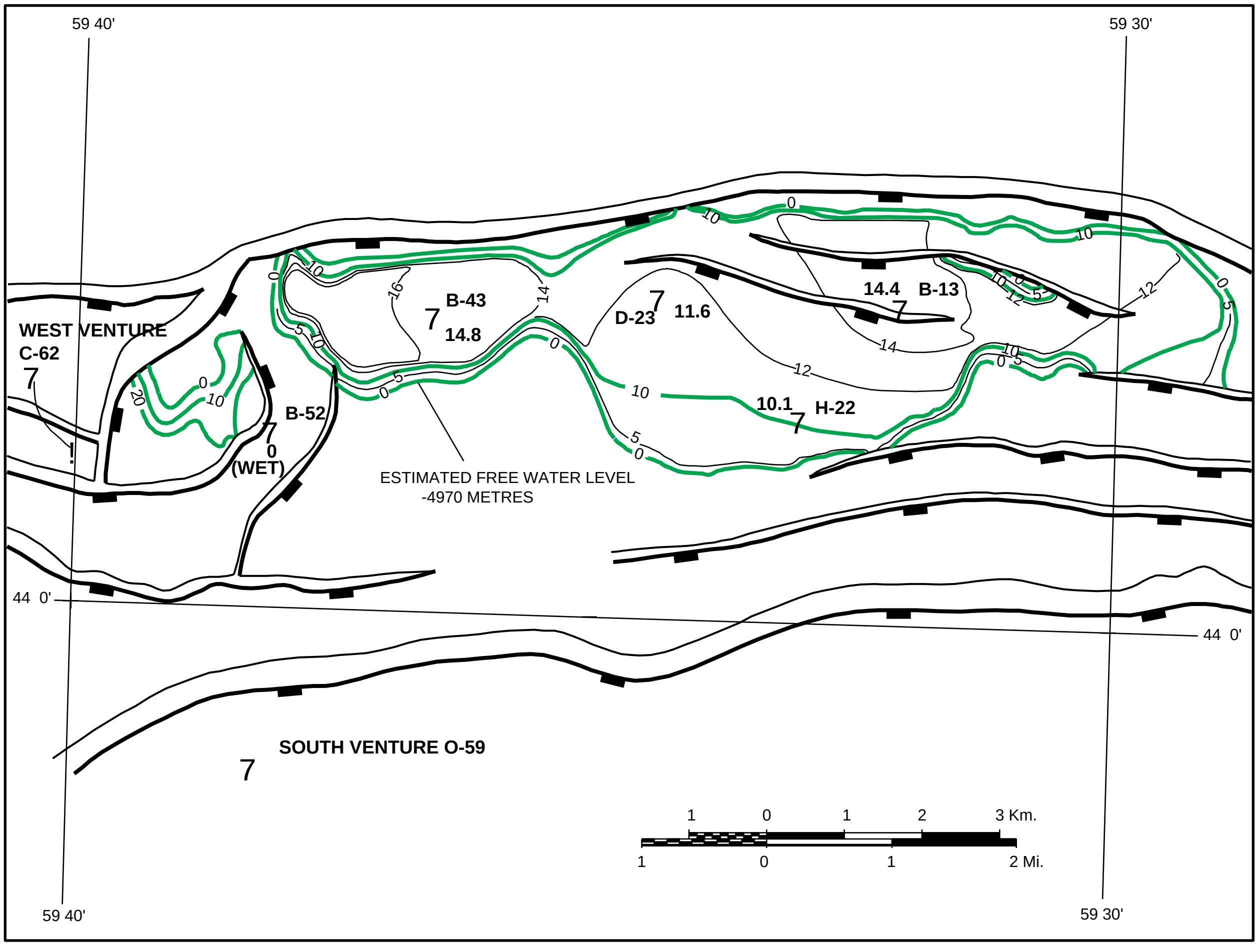

Figure 2.2.2.3.1: Venture Field - Sand 6 Upper Net Pay Thickness Map
Contour Interval: Variable, 2-10 metres

Detailed reservoir description studies of the Venture Field were conducted in 1985 and 1986 following the drilling of the H-22 well **(DPA - Part 2, Ref# 2.2.2.3.1 and 2.2.2.3.2)**. Gas accumulations were classified as major and minor sands on the basis of the size of the deterministic recoverable gas estimates. Four major sand reservoir accumulations were identified: the hydropressured Sand 2, and the overpressured Sands 3, 5, and 6 Upper. The general geological model used to construct reservoir thickness maps is of a north to south prograding delta complex. A consequent proximal to distal relationship is interpreted. Syndepositional movement on the north bounding fault is believed to influence sedimentation resulting in increased sand thickness northward toward the master fault.

2.2.2.4 Reservoir Zonation

The stratigraphic nomenclature for the reservoir section is shown in **Figure 2.2.2.4.1**, a schematic cross-section through the Venture Field. The naming convention assigned to these reservoir packages is applicable only to the Venture structure and wells drilled to the west of Venture within the same growth fault trend. There is good confidence in correlation of reservoir sandstone packages down to the 9 Limestone horizon. Confidence in correlation declines gradually with depth below this horizon due to reduced wellbore penetrations and reduced seismic data quality.

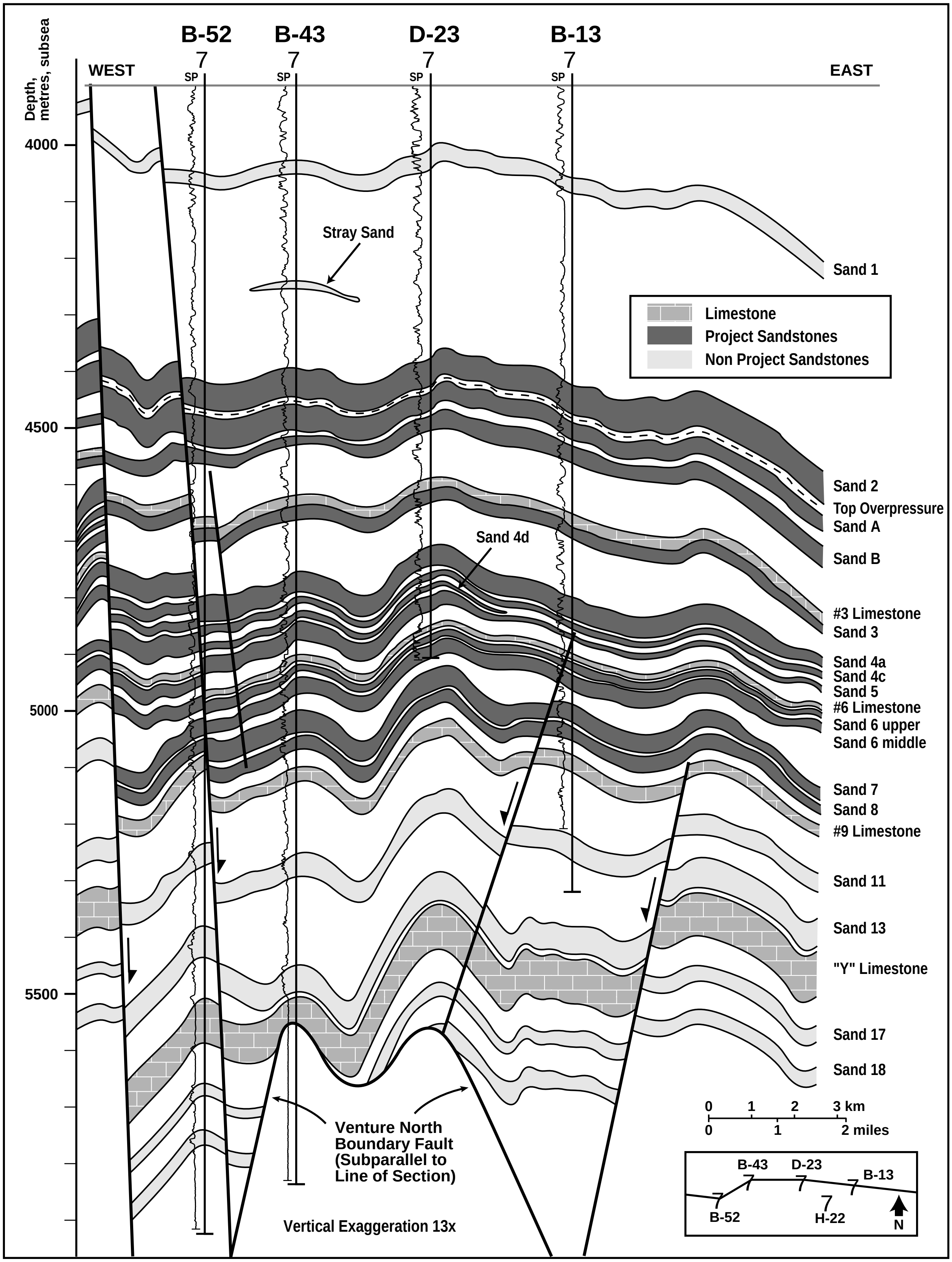

Figure 2.2.2.4.1: Venture Schematic Structural Cross-section

The deterministic reservoir studies conducted during the 1980's subdivided major sands into reservoir rock type layers for input to reservoir simulation models. The volumetrically significant minor sand reservoirs were mapped as single layers for input to simulation studies.

2.2.2.5 Geophysics

2.2.2.5.1 Seismic Database

The Venture Field is covered by many vintages of seismic data. A summary of acquisition and processing details for several of the datasets is included in **Table 2.2.2.5.1.1**. The data density and quality at the level of the major Sands (2, 3, 5, and 6) level is good to very good. Incorporated with the well data, the seismic generates a high level of confidence in the mapped intervals. Seismic continuity, frequency content and well control decreases, and mapping confidence declines slightly at depths below the 9 Limestone. The depth structure maps used for gas in place estimates are based on the 2D seismic data illustrated in **Figure 2.2.2.5.1.1.**

Table 2.2.2.5.1.1: Venture Acquisition and Processing Summary

Data Type	Survey Name	Incorp. In Study	Acq. Date	Acq. Style	Proc. Date	Field Kms	Proc. Details	Comments
2D	8624-M003-047E	Yes	1983	Marine Airgun-Digiseis Aquaflex-Digiseis	1983-84	356	60 fold Decon before and after stack, FD migration	Generally good to very good quality. Deteriorating with depth
2D	8624-M003-049E	Yes	1984	Marine Airgun-Digiseis Aquaflex-Digiseis	1984-85	121	60 fold Decon before and after stack, FD migration	Good to very good quality Deteriorating with depth
2D	8624-M003-45E	Yes	1982	Marine	1982-83	limited	60 fold DBS, DAS FK migration	Good quality data
2D	8620-S014-006E	No	1983	Marine	1983-84	42	60 fold Desig, Decon after stack, FD migration	Fair to good quality data, lower frequency
2D	8624-M003-041E	No	1981	Marine	1981-82	10	72 fold Desig, Decon after stack, FD migration	Good quality data, lower frequency
2D	8624-M003-035E	No	1980	Marine	1980-81	68	48 fold Desig, Decon after stack, FD migration	Generally good quality data, lower frequency
2D	8624-M003-033E	No	1979	Marine	1979-80	172	60 fold Decon before and after stack, FD migration	Fair to good quality, lower frequency

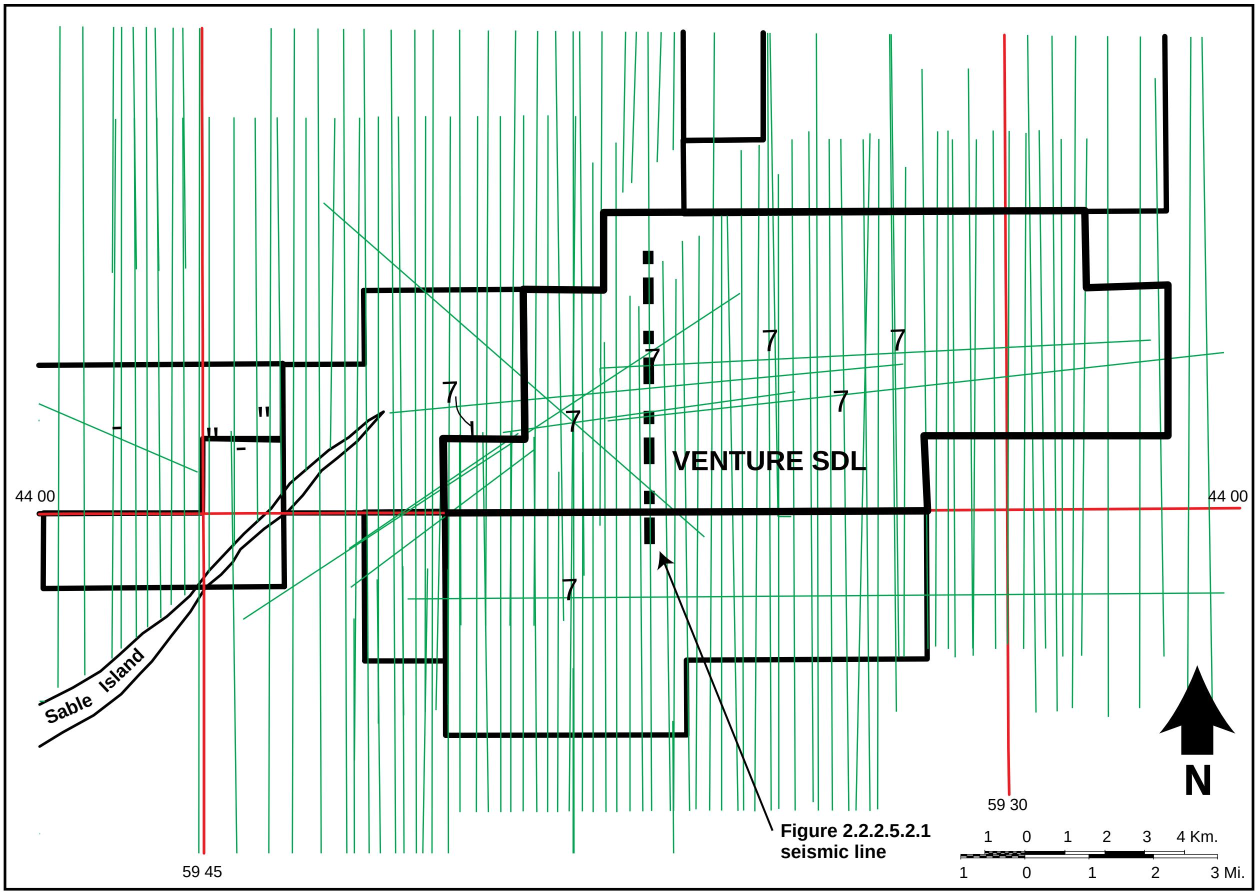

Figure 2.2.2.5.1.1: Venture Seismic Database Map

The maps used for gas in place (GIP) calculations at Venture are based on time and depth structure maps made in 1985 using the 1983 and 1984 datasets. The 1983 survey is the largest of the two and consists of 52 lines with a total of 356 line kilometres. The 1983 survey has only two strike lines over Venture. These strike lines, do however, run from west to east through the available well control. The dip lines have an east to west line spacing of approximately 300 metres over the crest and most of the flanks of the Venture structure. The extreme east and west flanks have a dip line spacing of approximately 600 metres. In the transition zone portion of this survey, data were successfully acquired via a radio telemetry, buoy-based system using airgun and aquaflex energy sources.

In 1984, a smaller combined standard marine and transition zone 2D survey was acquired to address the faulting associated with the B-52 well and to infill the flanking 600 metre dip line spacing.

2.2.2.5.2 Time Interpretation

The time and depth structure maps made in 1985 can be found in Part 2 of this submission (**DPA - Part 2, Ref. # 2.2.2.5.2.1 and 2.2.2.5.3.1**). This interpretation was generated primarily on paper sections that were hand timed, posted and contoured.

Checkshot survey corrected synthetic seismograms, generated at each well by convolving a minimum phase wavelet with an acoustic impedance series derived from wireline log sonic and density information, were used to tie well lithology to the seismic data. The B-52 VSP was also used to improve the well data to seismic reflector tie.

A number of horizons were picked and the 2 Sand, 3 Sand, 6 Limestone, 9 Limestone and Y Marker horizons were taken to final mapped form and used as the basis for the depth structure maps. The horizon markers at each of the wells are indicated in **Table 2.2.2.5.2.1**.

Table 2.2.2.5.2.1: Venture Horizon Markers

FIELD	VENTURE										OLYMPIA	
	D-23		B-43		B-13		B-52		H-22		A-12	
MAP HORIZON	Depth (M, ss)	TWT (sec)	Depth (M, ss)	TWT (sec)	Depth (M, ss)	TWT (sec)	Depth (M, ss)	TWT (sec)	Depth (M, ss)	TWT (sec)	Depth (M, ss)	TWT (sec)
#2 SANDSTONE	-4374.3	3079	-4389.2	3083	-4420.1	3110	-4415.8	NR	-4463.6	NR	-4339.0	NR
#3a Sand	-4612.0	3182	-4639.0	3195	-4680.2	3219	-4675.6	3200	-4678.3	3224	-4639.0	3042
#6 LIMESTONE	-4867.0	3303	-4916.0	3322	-4914.0	3342	-4988.0	3345	-4918.0	3329	-4959.0	NR
#9 LIMESTONE	NDE	NDE	-5100.9	3437	-5077.9	3440	-5102.6	Fault	-5063.8	3422	-4680.0	3222
" Y " LIMESTONE	NDE	NDE	NR	NR	NDE	NDE	-5506.6	3637	-5428.9	3610	-5040.0	NR

NDE - Not Deep Enough; NR - No Reflection

Several attribute projects and one principal component analysis were carried out after the Venture mapping project. The studies were based on a pseudo-3D seismic dataset generated from the 1983 2D survey. These studies supported the deterministic reservoir mapping, but results were restricted by the limited bandwidth and data quality of the seismic dataset. **Figure 2.2.2.5.2.1** is a representative seismic line illustrating data quality and structural geometry. The location of this line is shown as a bold dashed line on **Figure 2.2.2.5.1.1**.

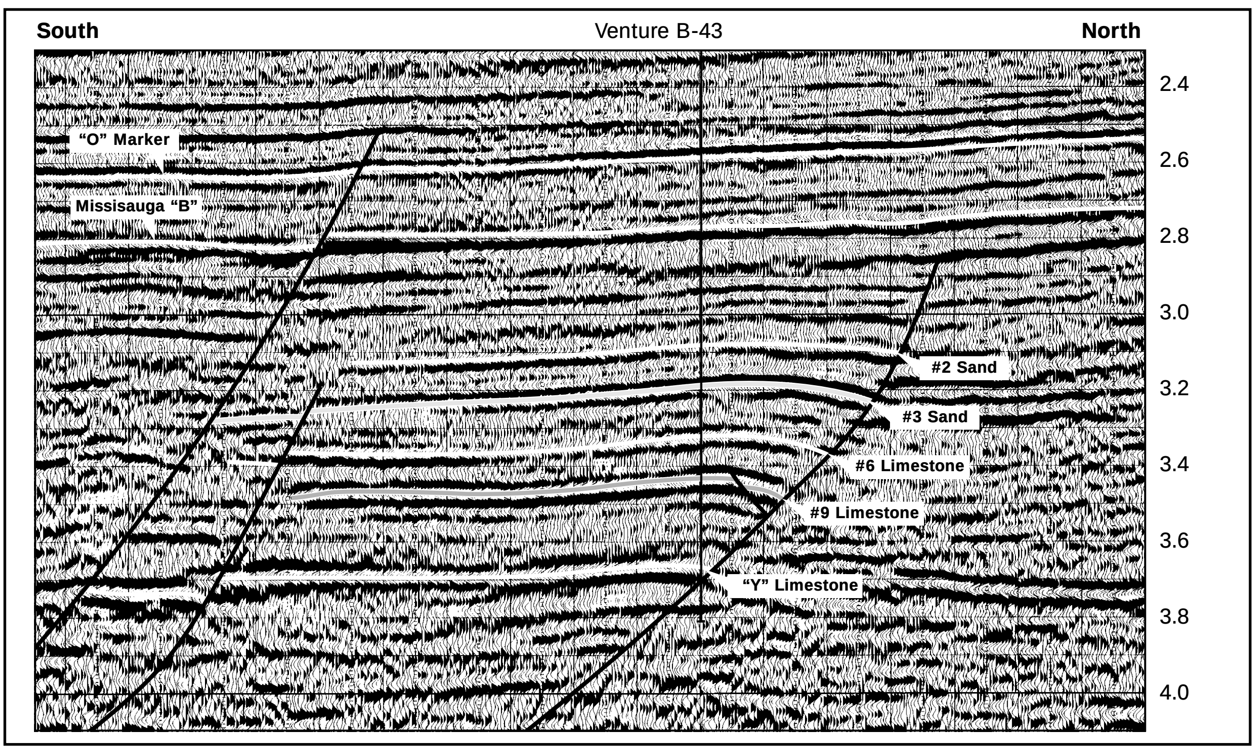

Figure 2.2.2.5.2.1 Venture Seismic Line

2.2.2.5.3 Depth Conversion

The method and details of the depth conversion technique used at Venture are documented in Part Two of this document (**DPA - Part 2, Ref. # 2.2.2.5.3.1**). The final depth conversion was completed in 1985 and incorporated the 1984 survey and adjacent well results into the time interpretation. Time structure maps for five horizons (2 Sand, 3 Sand, 6 Limestone, 9 Limestone and the Y Limestone) were digitized and gridded.

Velocity surveys from the five Venture wells, South Venture O-59 and Olympia A-12 (**Table 2.2.2.5.3.1**), were used to generate average velocity values to each of the mapped horizons.

Table 2.2.2.5.3.1: Venture Velocity Surveys

Well	Year Acquired	Checkshot Available	Checkshot Type	VSP Available	VSP Type
Venture D-23	1979	Yes	Vertical	No	NA
Venture B-13	1981	Yes	Vertical	No	NA
Venture B-43	1982	Yes	Vertical	No	NA
Venture B-52	1983	Yes	Vertical	Yes	Vertical
Venture H-22	1984	Yes	Vertical	No	NA
South Venture O-59	1983	Yes	Vertical	No	NA
West Venture C-62	1985	Yes	Deviated Well	No	NA
Olympia A-12	1983	Yes	Vertical	No	NA

The discrete points were then hand contoured for each horizon following trends present in the 1983 and 1984 2D seismic stacking velocity data. Seismic lag maps were generated for each time mapped horizon using values calculated at each well and used to time lag correct the time structure maps to the well velocity data. The gridded average velocity maps and the gridded corrected time structure maps were combined to create depth structure maps. Intermediate depth maps were generated from hand contoured wellbore thickness data.

2.2.2.6 Petrophysics

A detailed petrophysical evaluation of all five wells in the Venture Field was conducted using all available wireline log data, conventional/special core analysis data (**DPA - Part 2, Ref. # 2.2.2.6.1**), and pressure data. A detailed summary of the interpretation parameters and methodology is given in Part Two of this documents (**DPA - Part 2, Ref. # 2.2.2.6.2)**. The results of this evaluation are shown in **Tables 2.2.2.6.1 to 2.2.2.6.5**.

Table 2.2.2.6.1: Venture D-23 Project Reservoir Parameter Summary

Sand Unit	Measured Depth Top (m)	Measured Depth Base (m)	Elevation Top (m ss)	Elevation Base (m ss)	Gross Thickness (m)	Net Pay (m)	Average Porosity (%)	Average 'J' Sw (%)	Average Permeability* (mD)
2	4406.0	4452.6	-4374.3	-4420.9	46.6	15.7	11.1	34.3	2.8
A	4464.0	4497.0	-4432.3	-4465.3	33.0	0.0	-	-	-
B	4514.0	4541.0	-4482.3	-4509.3	27.0	7.3	13.7	50.0	0.6
3	4641.8	4665.0	-4610.1	-4633.3	23.2	16.3	19.9	41.4	21.3
4a&b	4747.0	4775.0	-4715.3	-4743.3	28.0	9.7	16.2	60.0	0.6
4c	4786.0	4801.0	-4759.3	-4769.3	10.0	5.8	15.1	36.7	0.6
4d	4811.0	4819.0	-4779.3	-4787.3	8.0	2.9	15.4	48.0	0.6
5	4829.2	4856.7	-4797.5	-4825.0	27.5	13.5	20.4	31.5	32.0
6u	4898.8	4912.5	-4867.1	-4880.8	13.7	11.6	21.2	31.8	65.6
6m	4916.2	4941.6	-4884.5	-4909.9	25.4	20.2	18.7	40.6	179.2
7	NDE	-	-	-	-	-	-	-	-
8	NDE	-	-	-	-	-	-	-	-

NDE - Not Deep Enough

* based on core analysis porosity vs permeability transforms

Table 2.2.2.6.2: Venture B-13 Project Reservoir Parameter Summary

Sand Unit	Measured Depth Top (m)	Measured Depth Base (m)	Elevation Top (m ss)	Elevation Base (m ss)	Gross Thickness (m)	Net Pay (m)	Average Porosity (%)	Average 'J' Sw (%)	Average Permeability* (mD)
2	4454.2	4505.4	-4420.1	-4471.3	51.2	27	14.4	39.4	62.5
A	4520.0	4552.0	-4485.9	-4517.9	32.0	9.1	13.7	60.0	0.6
B	4567.0	4602.0	-4532.9	-4567.9	35.0	9.8	14.8	62.3	1.0
3	4714.3	4738.8	-4680.2	-4704.7	24.5	6.7	19.1	76.4	38.3
4a	4833.0	4849.0	-4798.9	-4814.9	16.0	0.0	-	-	-
4c	4877.0	4891.0	-4842.9	-4856.9	14.0	10.5	14.8	55.0	26.5
4d	-	-	-	-	-	-	-	-	-
5	4897.0	4907.0	-4862.9	-4872.9	10.0	0.0	-	-	-
6u	4949.6	4964.0	-4915.5	-4929.9	14.4	14.4	18.7	39.4	47.3
6m	4969.2	4994.0	-4935.1	-4959.9	24.8	14.6	17.9	71.4	6.0
7	5017.0	5029.0	-4982.9	-4994.9	12.0	10.5	14.4	72.0	4.4
8	5057.0	5084.0	-5022.9	-5049.9	27.0	14.2	16.1	60.0	2.5

* based on core analysis porosity vs permeability transforms

Table 2.2.2.6.3: Venture B-43 Project Reservoir Parameter Summary

Sand Unit	Measured Depth Top (m)	Measured Depth Base (m)	Elevation Top (m ss)	Elevation Base (m ss)	Gross Thickness (m)	Net Pay (m)	Average Porosity (%)	Average 'J' Sw (%)	Average Permeability* (mD)
	(m)	(m)	(m ss)	(m ss)	(m)	(m)	(%)	(%)	(mD)
2	4423.3	4474	-4389.2	-4439.9	50.7	14.7	8.6	48	0.3
A	4487.0	4534.0	-4452.9	-4499.9	47.0	5.9	13.5	53.0	0.5
B	4543.0	4567.0	-4508.9	-4532.9	24.0	3.5	15.7	49.0	1.6
3	4673.1	4697.8	-4639.0	-4663.7	24.7	21.3	23.1	45.0	210.2
4a	4788.0	4806.0	-4753.9	-4771.9	18.0	7.3	17.2	57.0	1.0
4c	4832.0	4843.0	-4797.9	-4808.9	11.0	2.6	12.9	60.0	0.3
4d	4857.0	4870.0	-4822.9	-4835.9	13.0	5.8	19.7	47.0	2.3
5	4876.3	4909.7	-4842.2	-4875.6	33.4	12.3	18.6	35.4	25.7
6u	4950.0	4964.8	-4915.9	-4930.7	14.8	14.8	20.2	37.0	79.3
6m	4976.6	5002.8	-4942.5	-4968.7	26.2	7.1	20.6	70.0	21.0
7	5028.0	5060.0	-4993.9	-5025.9	32.0	11.3	15.9	49.6	25.6
8	5077.0	5101.0	-5042.9	-5066.9	24.0	13.4	18.6	37.0	9.5

* based on core analysis porosity vs permeability transforms

Table 2.2.2.6.4: Venture B-52 Project Reservoir Parameter Summary

Sand Unit	Measured Depth Top (m)	Measured Depth Base (m)	Elevation Top (m ss)	Elevation Base (m ss)	Gross Thickness (m)	Net Pay (m)	Average Porosity (%)	Average 'J' Sw (%)	Average Permeability* (mD)
2	4451.2	4499.6	-4415.8	-4464.2	48.4	0.0	-	-	-
A	4513.0	4568.0	-4477.6	-4532.6	55.0	0.0	-	-	-
B	4575.0	4601.0	-4539.6	-4565.6	26.0	0.0	-	-	-
3	4711.0	4734.9	-4675.6	-4699.5	23.9	12.2	19.2	79.4	13.6
4a	4836.0	4859.0	-4800.6	-4823.6	23.0	0.0	-	-	-
4c	4886.0	4901.0	-4850.6	-4865.6	15.0	0.0	-	-	-
4d	4920.0	4932.0	-4884.6	-4896.6	12.0	3.8	17.8	90.0	1.3
5	4944.3	4974.9	-4908.9	-4939.5	30.6	11.8	13.5	73.0	1.8
6u	5022.8	5047.2	-4987.4	-5011.8	24.4	0.0	-	-	-
6m	5064.1	5085.1	-5028.7	-5049.7	21.0	0.0	-	-	-
7	5113.0	5132.0	-5077.6	-5096.6	19.0	0.0	-	-	-
8	(faulted)	-	-	-	-	0.0	-	-	-

* based on core analysis porosity vs permeability transforms

Table 2.2.2.6.5: Venture H-22 Project Reservoir Parameter Summary

Sand Unit	Measured Depth Top (m)	Measured Depth Base (m)	Elevation Top (m ss)	Elevation Base (m ss)	Gross Thickness (m)	Net Pay (m)	Average Porosity (%)	Average 'J' Sw (%)	Average Permeability* (mD)
2	4502.0	4535.6	-4463.6	-4497.2	33.6	0	-	-	-
A	4546.0	4577.0	-4507.6	-4538.6	31.0	1.4	11.3	95.0	0.2
B	4594.0	4619.0	-4555.6	-4580.6	25.0	0.0	-	-	-
3	4716.7	4736.8	-4678.3	-4698.4	20.1	8.0	17.7	88.4	1.6
4a	4816.0	4833.0	-4777.6	-4794.6	17.0	1.4	11.0	95.0	0.1
4c	4861.0	4870.0	-4822.6	-4831.6	9.0	5.6	12.7	68.0	0.2
4d	4884.0	4891.0	-4845.6	-4852.6	7.0	0.0	-	-	-
5	4896.6	4920.0	-4858.2	-4881.6	23.4	0.0	-	-	-
6u	4957.5	4970.9	-4919.1	-4932.5	13.4	10.1	17.7	46.1	11.3
6m	4974.5	4998.2	-4936.1	-4959.8	23.7	6.8	17.4	90.2	1.9
7	5020.0	5033.0	-4981.6	-4994.6	13.0	12.2	17.2	52.0	19.2
8	5054.0	5079.0	-5015.6	-5040.6	25.0	6.1	18.3	58.0	1.3

* based on core analysis porosity vs permeability transforms

Zonal average porosity ranges from nine to 23 percent. The primary controls on porosity and permeability are average grain size, dissolution of unstable framework grains and the presence of early authigenic chlorite which inhibited the development of porosity occluding quartz-overgrowth cement. Water saturated microporosity associated with the grain-coating chlorite is believed responsible for the high irreducible water saturation values calculated in most overpressured gas sands.

Porosity was calculated from both density and sonic log measurements. Density porosity, calibrated to stressed core porosity measurements, was the preferred method. Where the density log measurements were of poor quality due to hole washout or gas effect, shale-corrected sonic log porosity was used.

The calculation of water saturation incorporated both wireline log data and capillary pressure data from core analysis. Although the two measurements compared favourably in most gas reservoirs, mud filtrate invasion in water bearing reservoirs was often deep enough to render the induction tools unreliable in the calculation of water saturation. Consequently, water saturation was determined primarily from capillary pressure data and the Leverett-J function equation (**DPA - Part 2, Ref. # 2.2.2.6.3**).

The Archie equation was used for wireline log water saturation calculations. Cementation and saturation exponents were determined from special core analysis measurements. True formation resistivity was determined from the deep induction measurement. Formation water resistivity was derived using a salinity gradient from DST formation water recoveries, and a formation temperature gradient determined from corrected bottom hole temperature measurements.

Net porous sand cutoff parameters were selected to correspond with a minimum permeability cutoff value of 0.1 mD to air at ambient conditions. A porosity cutoff value of 10 percent at in situ condition was generally found to be appropriate based upon drillstem tests and core analysis data. No water saturation cutoff was employed in the mapping of these reservoirs.

In only a few cases do existing wells intersect the gas/water contact. Consequently, free water levels were estimated using pressure data, and bracketing of the contacts from wireline log analysis and drillstem test results.

2.2.2.7 Gas in Place

Gas in place estimates for the Venture Field have been generated using deterministic and probabilistic methods. The probabilistic assessment of gas in place was conducted in 1995 and the methodology is described in detail in Part Two (**DPA - Part 2, Ref. # 2.2.2.7.1**). The summation of mean values from the output expectation curves generated for the 12 Project sands is 49.2 E9M3. Results of this probabilistic assessment for each of the Project sands are shown in **Table 2.2.2.7.1**.

Table 2.2.2.7.1: Venture Probabilistic Estimates of Gas In Place (E9M3)

Reservoir Sandstone	P90	P50	P10	Mean
2	2.5	6.2	12.2	**7.0**
A	0.2	0.8	2.1	**1.0**
B	0.5	1.4	3.3	**1.7**
3	2.9	5.9	11.1	**6.5**
4a	0.4	1.0	3.0	**1.4**
4c	0.5	1.4	3.7	**1.8**
4d	0.3	1.0	3.5	**1.6**
5	1.8	5.0	12.2	**6.2**
6u	4.6	9.1	16.8	**10.1**
6m	2.2	4.8	10.1	**5.6**
7	1.0	2.4	5.5	**2.9**
8	1.2	2.9	6.2	**3.4**
Project Total	18.1	41.9	89.7	**49.2**

Deterministic reservoir maps of the Venture Field were generated in 1985 and 1986. Gas in place estimates for Project sands are shown in **Table 2.2.2.7.2** and represent unrisked volumes.

Table 2.2.2.7.2: Venture Deterministic Estimates of Gas In Place (E9M3)

Reservoir Sandstone	Gas in Place
2	15.2
A	1.8
B	2.7
3	9.7
4a	2.1
4c	1.5
4d	2.2
5	10.3
6u	12.9
6m	4.3
7	3.7
8	4.7
Total	71.1

Structure maps were constructed for each reservoir sandstone based on the seismic depth maps generated at five seismic horizons. A reservoir map suite was constructed for each rock type in the four major sands and the 6 Middle Sands. The reservoir map suite consists of a structure map, a gross thickness map, a net-to-gross ratio map, an isoporosity map, and an isopermeability map. The same reservoir map suite was constructed for the following minor reservoir Sandstones; A, B, 4a, 4c, 4d, 7, 8, and the deep Sand 11 accumulation. Remaining minor gas accumulations were commonly encountered in only one well. In these cases, single well areal assignments were applied for deterministic calculation, or, as with Sand 1, a prior 1984 generation map suite was used. Individual reservoir and rock type maps are included in Part Two (**DPA - Part 2, Ref .# 2.2.2.3.1, 2.2.2.3.2, & 2.2.2.6.3**).

Some minor gas accumulations in the Venture Field are not currently included in the Project. Predominantly, these are deep overpressured sands below the 9 Limestone horizon. The larger of these accumulations, in Sands 11 and 13, have mean probabilistic gas in place estimates of 1.9 and 1.2 E9M3, respectively. These horizons are not included in the development plan because of their estimated small volumes and associated projected high drilling and production costs.

2.2.3 NORTH TRIUMPH FIELD

2.2.3.1 Field History

The North Triumph Field was discovered in 1986 (**DPA - Part 2, Ref. # 2.2.3.1.1**). The discovery well, North Triumph G-43, encountered hydropressured gas in sands at the top of the Missisauga Formation. Gas was tested at rates between 991 to 1047 E3M3/d. Follow-up drilling consists of one downdip appraisal well, North Triumph B-52. This well encountered the gas/water contact of the single gas pool comprising the field. **Figure 2.2.3.1.1** illustrates the structure at the top of the gas bearing Missisauga Formation in North Triumph.

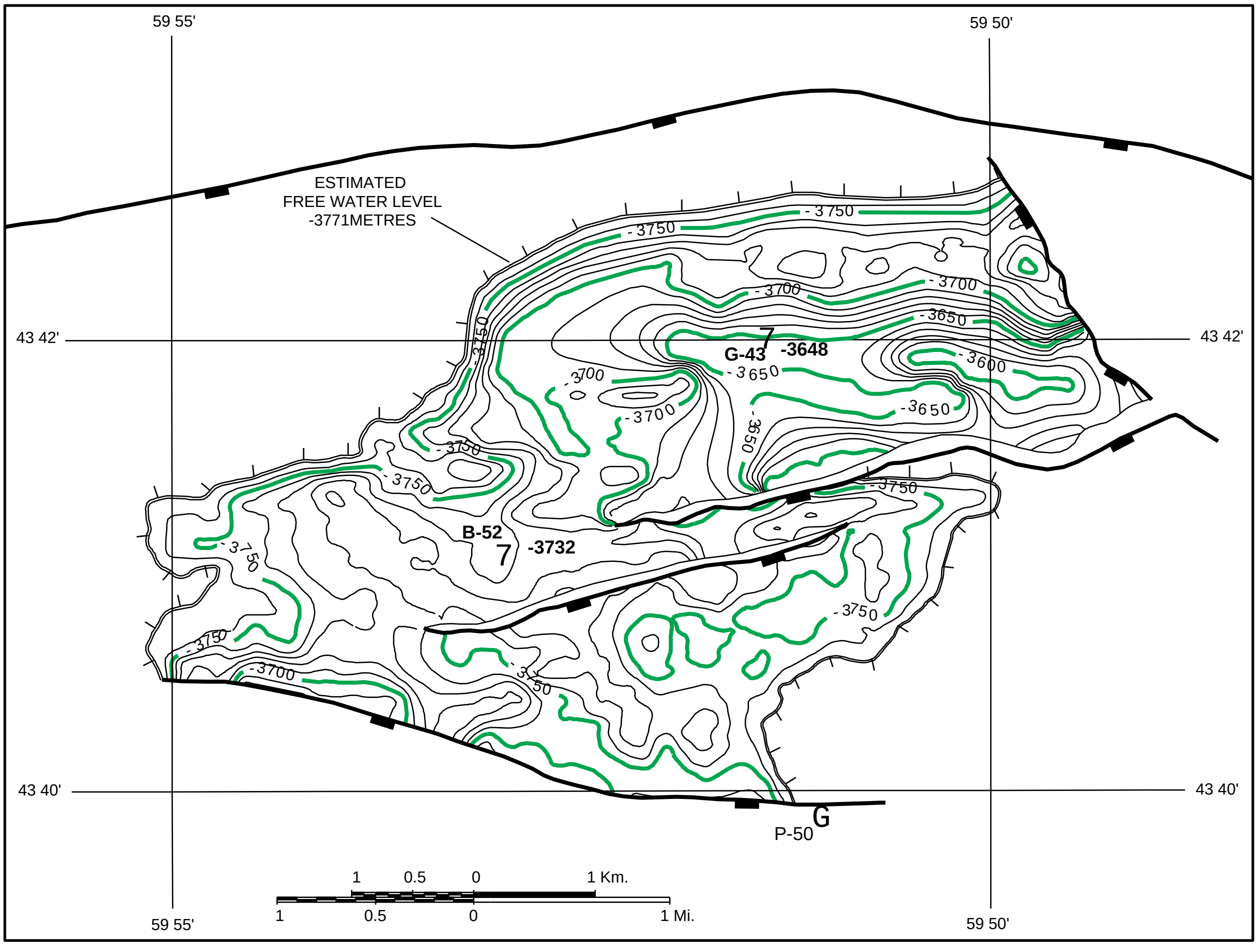

Figure 2.2.3.1.1: North Triumph - Top Missisauga Depth Structure Map
Contour Interval: 10 metres

2.2.3.2 Structural Configuration

The North Triumph structure consists of a rollover anticline bounded to the north and south by major listric growth faults. The north bounding fault downdrops to the south, and the top Missisauga level is offset by 600 to 650 metres. The southern boundary of the structure is marked by a fault system which drops the top Missisauga down to the south by as much as 1250 metres. Internally, the rollover anticline is partially dissected by two lesser en-echelon faults (**DPA - Part 2, Ref. # 2.2.3.2.1**). The field lies at a depth of 3640 metres subsea and extends over an area of 19 square kilometres.

Simple closure is provided to the north by rollover into the governing growth fault, and to the west by plunge of the anticline. Cross-fault seal is present to the east due to juxtaposition of the Upper Missisauga reservoir sands with Verrill Canyon shales. Cross-fault and/or fault-smear seal occurs across the southern bounding fault, where the Upper Missisauga reservoir sands are juxtaposed with interbedded sands and shales of the lower Logan Canyon Formation.

2.2.3.3 Geology

Hydropressured gas is trapped in a single pool within stacked sandstones in the uppermost part of the Missisauga Formation. Structural mapping indicates a gas column of 171 metres extending from the crest of the rollover anticline to the gas/water contact intercepted in the B-52 well.
The gas-bearing uppermost 100 metres of the Missisauga Formation consists of an upward coarsening and cleaning succession which is shale-dominated at its base, with an increasing sandstone content upward. This succession represents deposition from a prograding delta complex. It is composed of a number of smaller scale coarsening and cleaning upward cycles which resulted from progradation of successive individual delta lobes into the area. Log correlation of these cycles is good between the two wells, indicating stratigraphic continuity over most, if not all, of the North Triumph structure (**DPA- Part 2, Ref. # 2.2.3.3.1 through 2.2.3.3.3**). Pressure data also indicates continuity of these sandstones between the wells.

The reservoir development model implemented in the feasibility stage of this Project and used for gas in place determination at North Triumph is one of a north to south thinning wedge. This model combines the effects of a northerly source for the sands with syndepositional downward movement on the northern bounding growth fault. The latter acts to trap most of the reservoir quality sand in the northern portion of the field. According to this model, reservoir development decreases from a maximum of 45 meters adjacent to the northern bounding fault, to 38 meters at G-43, and thins linearly to 23 meters at the B-52 well. Thickness is then held constant to the southern extent of the field.

Convolution of this model with the structure map and recognized gas/water contact at -3771 m SS permits construction of a net pay map (**Figure 2.2.3.3.1**).

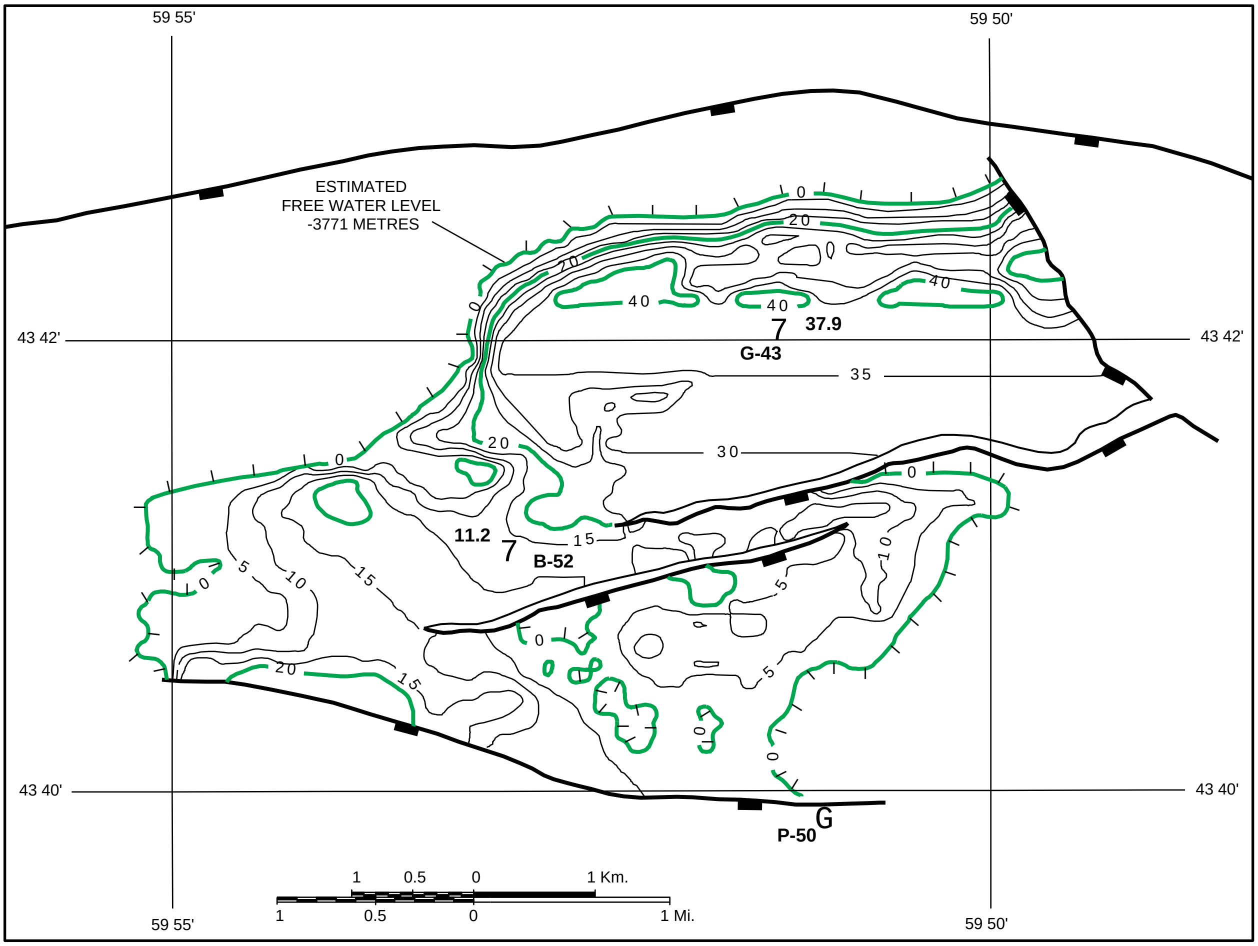

Figure 2.2.3.3.1: North Triumph - Net Pay Map
Contour interval 5 metres

2.2.3.4 Reservoir Zonation

The sands containing gas in the North Triumph Field are in pressure communication, so there has been no need to subdivide the reservoir section into different zones. The single gas pool is termed the A Pool. It lies within a 100 metre thick, coarsening-upward, shale-to-sandstone succession, which is termed the A Reservoir Zone. This is illustrated in **Figure 2.2.3.4.1**. In the initial modeling of the recoverable gas reserves, the reservoir interval has been internally subdivided into 'flow units' on the basis of petrophysical attributes and a detailed facies model (**DPA - Part 2, Ref. # 2.2.3.3.3 & 2.2.1.3.3**).

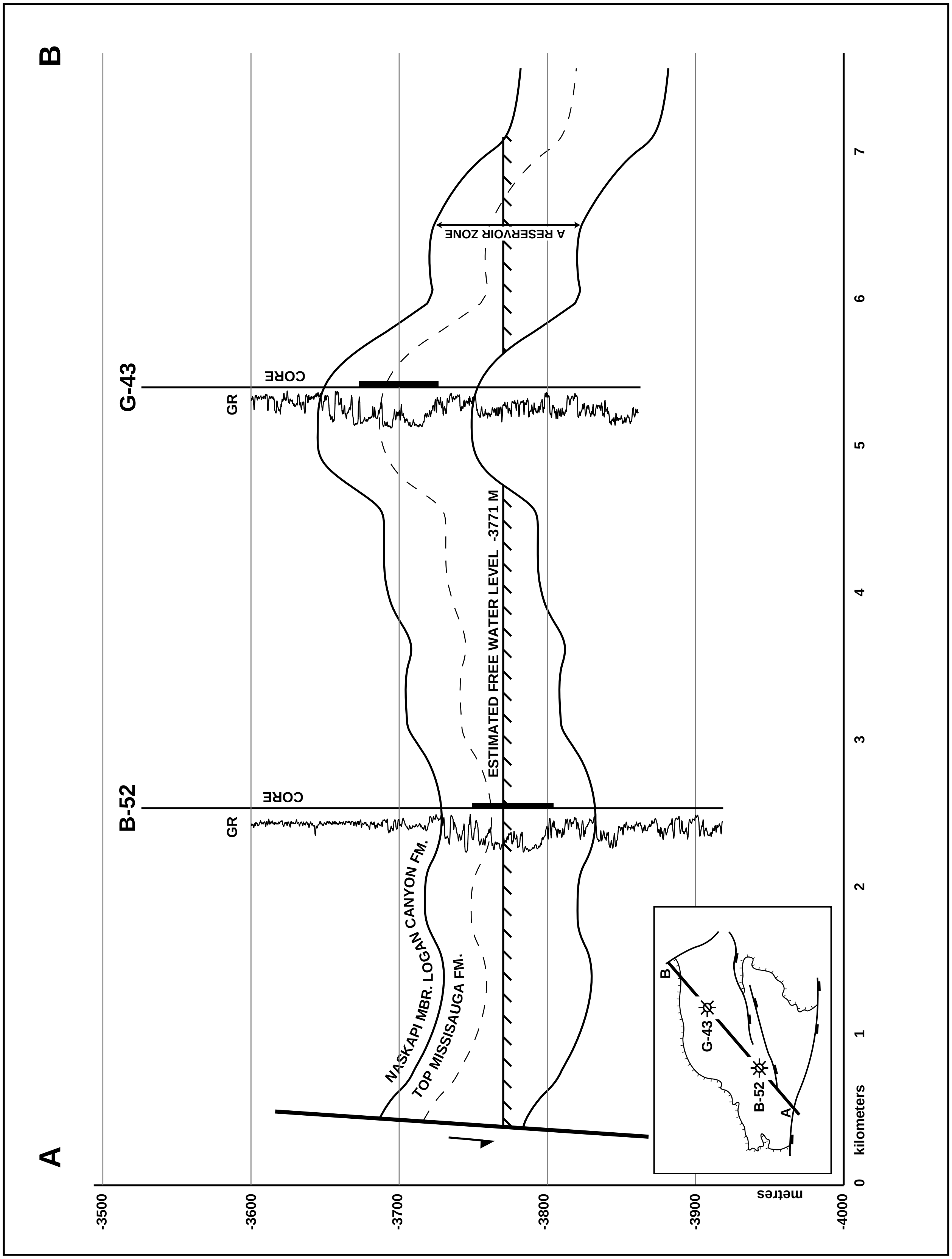

Figure 2.2.3.4.1: North Triumph Schematic Structural Cross-section

2.2.3.5 Geophysics

2.2.3.5.1 Seismic Database

The depth structure map used for gas in place estimation is based on an integration of 2D and reconnaissance 3D seismic data, as illustrated in **Figure 2.2.3.5.1.1.** The 2D data were acquired in the period from 1980 to 1982 and were processed with a standard marine runstream. These data exhibit fair data quality down to the objective Missisauga level.

The reconnaissance 3D survey which covers part of the North Triumph structure has an areal extent of 260 square kilometres. It was acquired in 1985 and purchased by Shell in 1987. It was incorporated into the interpretation in 1991. Data quality is generally better than that of the 2D data, and this results in improved fault resolution. Because the 3D survey was acquired with 100 metre in-line spacing, it required bin interpolation prior to cross-line migration. Both the 2D and reconnaissance 3D data were used to map the structural configuration of the North Triumph Field. A summary of acquisition and processing details is included in **Table 2.2.3.5.1.1.**

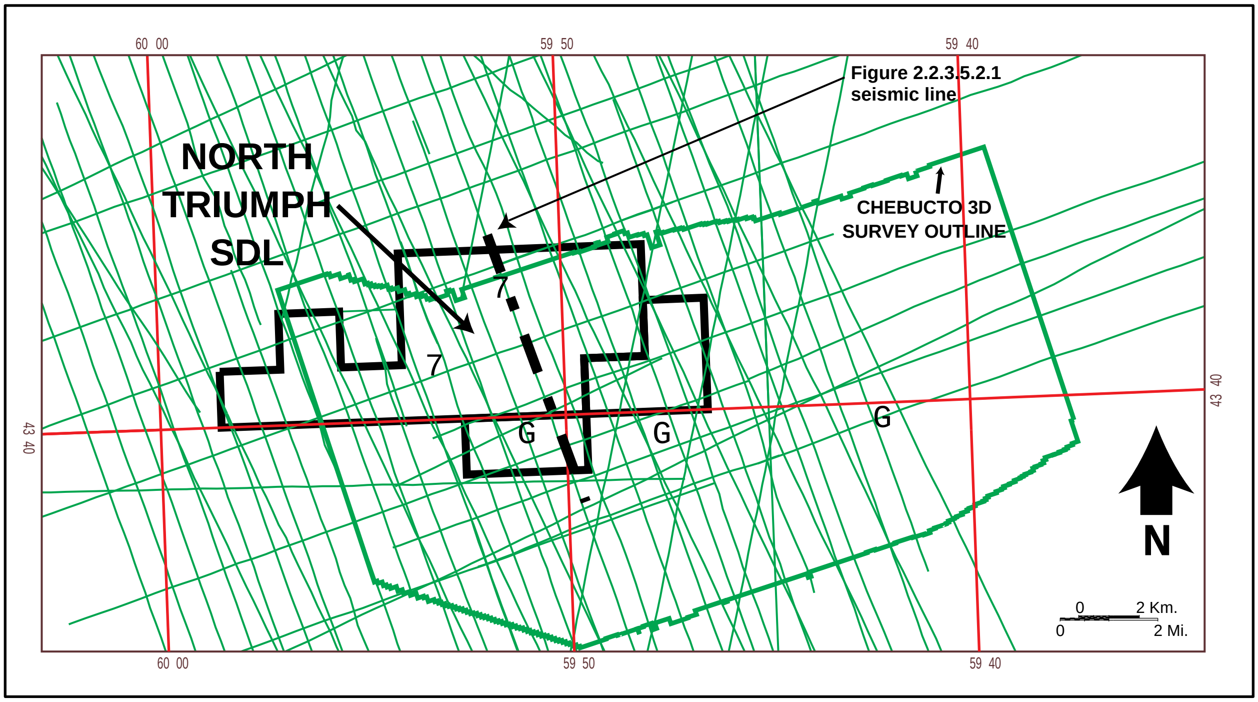

Figure 2.2.3.5.1.1: North Triumph Seismic Database Map

Table 2.2.3.5.1.1: North Triumph Acquisition and Processing Summary

Data Type	Survey Name	Incorp. In Study	Acq. Date	Acq. Style	Proc. Date	Field Kms	Proc. Details	Comments
2D	050E series	No	1987	Marine	1988	200	60 Fold, Desig, FK Migration	Generally good to very good quality data
2D	048E Series	No	1985	Marine	1985	92	54 Fold, Desig, FK Migration	Generally good quality data
3D Partial	010e Series	Yes	1985	Marine	1985	2685	64 Fold, DMO, FD Migration	Generally fair to good data quality
2D	004E Series	Yes	1983	Marine	1983	22	40 Fold Desig, FD Migration	Generally poor to fair quality
2D	033E Series	Yes	1982	Marine	1983	738	54 Fold, Desig,FD Migration	Generally poor to fair quality
2D	027E Series	Yes	1981	Marine	1981	320	60 Fold, Desig,FD Migration	Generally poor data quality
2D	023E Series	Yes	1980	Marine	1980	315	48 Fold, Desig, FD Migration	Generally poor to fair data quality
2D	020 E Series	No	1976	Marine	1976	36	24 Fold,No Mig	Generally poor to fair data quality

2.2.3.5.2 Time Interpretation

Synthetic seismic traces, based on convolving a zero phase wavelet with an acoustic impedance series derived from wireline log sonic and density information, were used to tie lithology to the seismic data.

The 3D seismic data were interpreted using a Landmark™ workstation and provide the basis for the time and depth structure maps. The 2D data were manually interpreted and provide structural control on the northern flank of the feature where there is no 3D coverage. The top Missisauga correlated from well control was picked as the main mapping horizon and was used to define the structure of the main pool (shown in **Table 2.2.3.5.2.1)**. Greater spatial resolution of the reconnaissance 3D yielded better fault imaging than the 2D dataset and indicated two small displacement faults which partially bisect the anticlinal structure. A representative seismic line is illustrated in **Figure 2.2.3.5.2.1** and is indicated by a bold dashed line on **Figure 2.2.3.5.1.1**.

Table 2.2.3.5.2.1: North Triumph Horizon Markers

FIELD	North Triumph							
	G-43				B-52			
MAP HORIZON	Depth MD (m)	Depth TVD (m)	Depth M,ss	TWT (sec)	Depth MD (m)	Depth TVD (m)	Depth M,ss	TWT (sec)
Eocene Chalk	1379	1378	-1354	1.407	1428	1428	-1404	1.437
Wyandot Chalk	1628	1627	-1603	1.609	1658	1658	-1634	1.618
Top L. Logan Can.	2316	2315	-2291	2.066	2333	2333	-2309	2.054
Naskapi	3489	3407	-3383	2.664	3407	3407	-3383	2.654
Missisauga	3778	3672	-3648	2.801	3756	3756	-3732	2.829

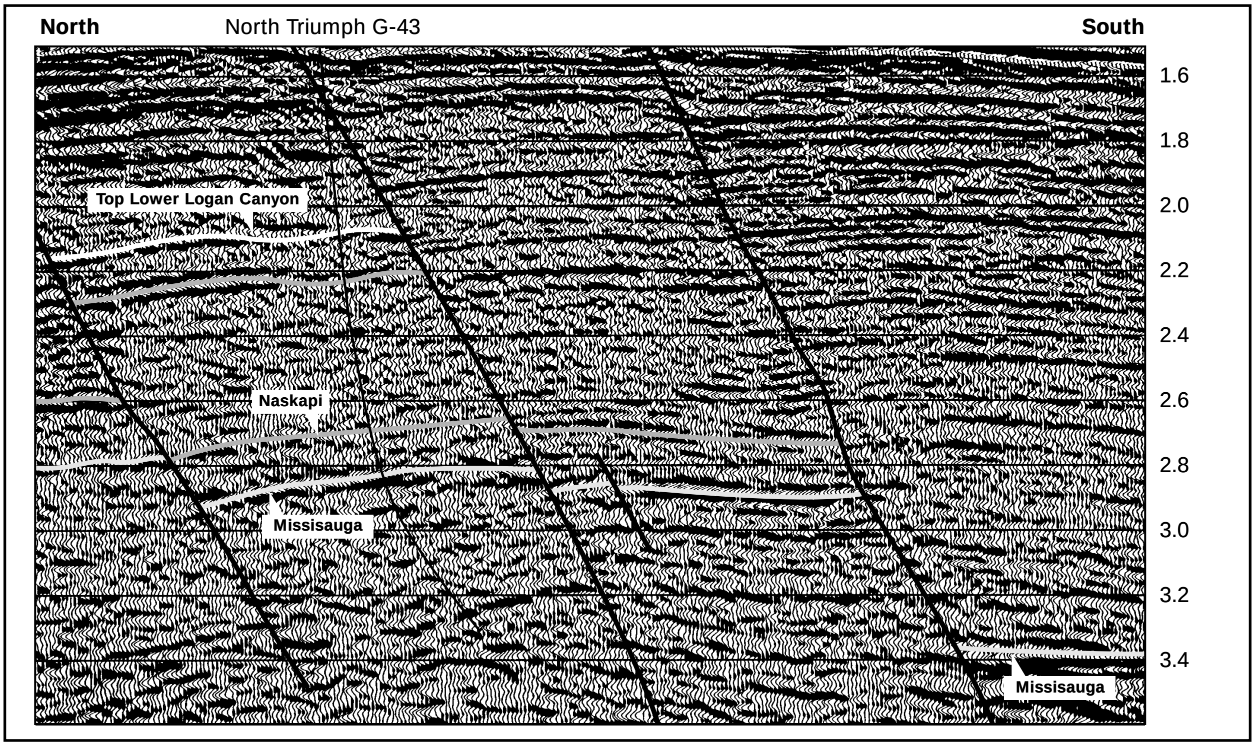

Figure 2.2.3.5.2.1: North Triumph Seismic Section

2.2.3.5.3 Depth Conversion

Time to depth conversion of the North Triumph Field is reviewed in Part Two of this document **(DPA - Part 2 Ref. # 2.2.3.5.3.1).** Depth conversions in the mid to late 1980's used a 'layer cake' methodology with a constant velocity from the seafloor to Wyandot marker. Local well control (**Table 2.2.3.5.3.1**) was used to generate time-depth functions for the Wyandot to mapped horizon interval.

Table 2.2.3.5.3.1: North Triumph Well Velocity Data

Well	Year Acquired	Checkshot Available	Checkshot Type	VSP Available	VSP Type
North Triumph G-43	1983	Yes	Vertical	No	NA
North Triumph B-52	1984	Yes	Vertical	No	NA

2.2.3.6 Petrophysics

Petrophysical evaluation of the two wells in the North Triumph Field used all available log data, extensive conventional/special core analysis data, and pressure data**.** A detailed summary of the interpretation parameters and methodology is given in Part Two of this document (**DPA - Part 2, Ref. # 2.2.3.6.1**). The results of this evaluation are in **Table 2.2.3.6.1**.

Table 2.2.3.6.1: North Triumph Reservoir Parameter Summary

North Triumph B-52 K.B. 24.0 Metres

Sand Unit	Measured Depth Top (m)	Measured Depth Base (m)	Elevation Top (m ss)	Elevation Base (m ss)	Gross Thickness (m)	Net Pay (m)	Average Porosity (%)	Average Sw (%)	Average Permeability* (mD)
A	3756.5	3858.5	-3731.9	-3834.5	102.6	11.2	18.0	36.0	60.0

North Triumph G-43 (deviated well) K.B. 24.0 Metres

Sand Unit	Measured Depth Top (m)	Measured Depth Base (m)	Elevation Top (m ss)	Elevation Base (m ss)	Gross Thickness (m)	Net Pay (m**)	Average Porosity (%)	Average Sw (%)	Average Permeability* (mD)
A	3778.0	3882.5	-3647.9	-3752.5	104.5	37.9	20.0	15.0	70-300

* Estimated from DST

** metres along hole

Pressure and test data from the two wells indicate that the North Triumph Field features a single pool of hydropressured gas. This is reservoired in the uppermost sandstones of the Missisauga Formation. These data are in agreement with a gas/water contact encountered in the more down-dip well, B-52, at 3771 metres subsea. The crest of the North Triumph structure is mapped at 3600 metres subsea, giving a total gas column of 171 metres. Net pay varies between the two wells due to changes in structural position and minor variation in reservoir development. The G-43 well contains 38 metres of net pay. The structurally lower B-52 well contains 11 metres. Net porous sand thickness was determined based on a permeability cutoff of 0.5 mD to air at ambient conditions. This was found to correspond to an in situ porosity value of 10 percent. A water saturation cutoff of 60 percent was used in the determination of net pay.

Zonal average porosity of the reservoir ranges from 19 to 20 percent. Zonal average permeabilities range from 60 to 300 mD. The primary control on porosity and permeability is average grain size. Porosity was calculated from density calibrated to stressed core porosity measurements. Zonal average water saturation of the reservoir ranges from 17 to 38 percent.

Water saturation for values used in the estimation of gas in place was calculated using the Archie equation. Cementation and saturation exponent values were based on special core analysis. Formation water resistivity was derived from RFT and DST fluid sample analysis, and a formation temperature gradient determined from bottom hole temperature measurements. Irreducible water saturations, as calculated from logs, range from six to 10 percent.

2.2.3.7 Gas in Place

The ranges of uncertainty of the parameters utilized in the probabilistic assessment of gas in place are detailed in Part Two (**DPA - Part 2, Ref. # 2.2.3.7.3)**. The results for the North Triumph Field are presented in **Table 2.2.3.7.1**.

Deterministic gas in place estimates, performed in 1990 and 1991, utilized average reservoir porosity and water saturation values determined from well petrophysics, an average net pay value as determined from the net pay map, and what was then considered the ‘most likely’ structure map for the area of the pool. The methodology of this deterministic gas in place estimation is presented in detail in Part Two (**DPA - Part 2, Refs #2.2.3.7.1 and 2.2.3.7.2**). The result is presented in **Table 2.2.3.7.2**. The deterministic volume is similar to the P50 and Mean values obtained from the probabilistic method.

Table 2.2.3.7.1: North Triumph Probabilistic Estimate of Gas In Place

Reservoir Sandstone	P90	P50	P10	Mean (E9M3)
Project Total	6.2	14.2	25.2	**15.2**

Table 2.2.3.7.2: North Triumph Deterministic Estimate of Gas In Place

Reservoir Sandstone	Gas in Place (E9M3)
A	15.8